光学学报

横向光力最新研究进展(特邀)

施宇智[1,2,3,4*],赖成兴[1,2,3,4],夷伟成[1,2,3,4],黄海洋[1,2,3,4],冯超[1,2,3,4],何涛[1,2,3,4],刘爱群[5],仇成伟[6],王占山[1,2,3,4], 程鑫彬[1,2,3,4**]

[1]同济大学物理科学与工程学院, 同济大学精密光学工程技术研究所, 上海 200092;
[2]先进微结构材料教育部重点实验室, 上海 200092;
[3]上海市数字光学前沿科学研究基地, 上海 200092;
[4]上海市全光谱高性能光学薄膜器件及应用专业技术服务平台, 上海 200092;
[5]香港理工大学电机与电子工程学系, 香港 999077;
[6]新加坡国立大学电气与计算机工程系, 新加坡 117583

摘要 光镊技术利用光和物质之间动量交换产生的光力对细小颗粒进行操控,具有无接触、操控尺寸小、精度高等特点,在基础物理、量子计算、生物医学等领域得到了广泛的应用。其中,横向光力(也称光横向力,OLF)是一种垂直于光的传播方向且与场强度梯度无关的特殊光力。近十年来,OLF的理论研究和实验探索成为了热点课题,在手性颗粒等超精密分选、光动量探测等方面有重要应用。从OLF的原理和产生条件、不同物理机制,以及在生物医学和物理化学等领域的应用等方面出发,对OLF的发展进行回顾和讨论,并对新的产生机制和更多的潜在应用与挑战进行展望。

关键词 横向光力; 角动量; 光学操控; 光学自旋; 手性颗粒

中图分类号 O439; TN256 **文献标志码** A **DOI:** 10.3788/AOS231739

1 引 言

动量是电磁波、声波、流体波、物质波等波场的重要属性,它可以表现为线性动量和角动量。光子作为电磁波的载体,也具有这两种动量,光子可以与物质产生相互作用,从而实现光学操控。其中,利用光子与颗粒的动量传递产生光力从而对颗粒进行操控的技术被称为“光镊”技术,它是Ashkin等[1]在20世纪70到80年代创立并发展的一种光学技术。光镊技术在捕获和操控微观颗粒方面具有独特的优势,它为生物医学、物理学、化学等领域的研究提供了新的手段。1997年,Steven Chu(朱棣文)、Claude Cohen-Tannoudji 和William D. Phillips三人因利用光力实现原子冷却获得诺贝尔物理学奖。2018年,Arthur Ashkin教授因其所发明的光镊及光镊技术在生物医学领域应用的突出贡献而荣获1/2诺贝尔物理学奖[2-7]。

光子与物质相互作用时会传递线性动量和角动量,从而在物质上施加光力[8-10]。常见的光力包括光梯度力(OGF)和光辐射压力。对于传统的高折射率颗粒来说,OGF方向与光强度梯度的方向一致并指向光强较大的点,而光辐射压力的方向通常与光的传播方向一致,太阳帆就是利用该原理的一个典型例子。在某些特殊情况下,光力方向可以与光传播方向相反,形成奇异“光牵引力”。光牵引力的产生与光场和颗粒的结构、性质,以及不同介质之间的线性动量变化等因素有关。例如,利用结构光束[11-14]、结构颗粒[15-17]、表面等离极化激元(SPP)[18-21]、超表面[22, 23]、谐振腔[24, 25]等方法都可以构建光牵引力。另一种垂直于光传播方向且与场强度梯度无关的特殊光力称为“横向光力(OLF)”,该力为本文的主要讨论对象,在颗粒分选、手性传感、动量检测等方面得到了广泛应用。

本文将回顾目前OLF在理论与实验方面的研究进展,并按照OLF不同的产生机制对其进行分类介绍。首先分别从实验和理论两个方面介绍目前产生OLF的一些代表性机制,包括横向自旋动量(也称为Belinfante自旋动量,BSM)、手性、自旋-轨道相互作用

收稿日期: 2023-11-03; **修回日期**: 2023-12-12; **录用日期**: 2023-12-21; **网络首发日期**: 2023-12-23

基金项目: 国家自然科学基金(61925504, 62192770, 61621001, 62205246, 62020106009, 6201101335, 62205249, 62192772, 62111530053)、上海市科学技术委员会科技计划(17JC1400800, 20JC1414600, 21JC1406100, 22ZR1432400)、上海市教育委员会“曙光”计划(17SG22)、上海市级科技重大专项-人工智能基础理论与关键核心技术(2021SHZDZX0100)、中国博士后科学基金(2022M712401)

通信作者: *yzshi@tongji.edu.cn; **chengxb@tongji.edu.cn

(SOI)、虚 Poynting 动量(IPM,即 Poynting 动量的虚部),以及诸如热、电、气泡等其他效应;然后介绍基于 OLF 的代表性应用,如微纳机器人、颗粒分选,以及一些生物医学和物理化学的应用;最后,对 OLF 的研究与发展进行总结,并对未来可能出现的新的物理机制和更多的应用领域进行展望。

2 光动量与横向光力简介

2.1 光动量

光的角动量包括自旋角动量(SAM)和轨道角动量(OAM)。1909 年,Poynting[26]发现圆偏振光(CPL)具有动量为 $\pm\hbar$ 的 SAM。1992 年,Allen 等[27]基于拉盖尔-高斯光束提出了 OAM 的概念,并引发了一系列基于 OAM 的应用研究。这种内在 OAM 与坐标原点和偏振起点无关,它平行于光束传播方向,被称为纵向 OAM。相比之下,外在角动量是一种与坐标原点和光束运动轨迹有关的角动量,它垂直于光束传播方向,类似于经典粒子的力学角动量,可以表示为 $\boldsymbol{L}\propto\boldsymbol{r}\times\boldsymbol{p}$,其中 $\boldsymbol{L}$ 为角动量,$\boldsymbol{r}$ 为径向矢量,$\boldsymbol{p}$ 为动量。这种外在角动量可被认为是一种横向 OAM。

在电动力学中,光的时间平均动量密度在介电常数为 ε 和磁导率为 μ 的介质中可以被分为自旋和轨道两部分,具体表达式[28-31]为

$$\boldsymbol{p}=\boldsymbol{p}_{\mathrm{s}}+\boldsymbol{p}_{\mathrm{o}}, \tag{1}$$

其中,对应的自旋项与轨道项又可以分别表示为

$$\boldsymbol{p}_{\mathrm{s}}=\frac{1}{2}\nabla\times\boldsymbol{S}=\frac{\mathrm{Im}\left[\nabla\times\left(\varepsilon\boldsymbol{E}^{*}\times\boldsymbol{E}\right)+\nabla\times\left(\mu\boldsymbol{H}^{*}\times\boldsymbol{H}\right)\right]}{8\omega}, \tag{2}$$

$$\boldsymbol{p}_{\mathrm{o}}=\frac{\mathrm{Im}\left[\varepsilon\boldsymbol{E}^{*}\cdot(\nabla)\boldsymbol{E}+\mu\boldsymbol{H}^{*}\cdot(\nabla)\boldsymbol{H}\right]}{4\omega}, \tag{3}$$

式中:$\boldsymbol{E}$ 和 $\boldsymbol{H}$ 分别为电场强度和磁场强度;$\boldsymbol{E}^{*}$ 和 $\boldsymbol{H}^{*}$ 分别为 $\boldsymbol{E}$ 和 $\boldsymbol{H}$ 的共轭;ω 为 CPL 的角频率。其中,定义 $\boldsymbol{A}^{*}\cdot(\nabla)\boldsymbol{A}=\sum_{i=x,y,z}A_i^{*}\nabla A_i$,自旋项中的 $\boldsymbol{S}$ 为 SAM 的密度,具体表达式为

$$\boldsymbol{S}=\frac{\mathrm{Im}\left(\varepsilon\boldsymbol{E}^{*}\times\boldsymbol{E}+\mu\boldsymbol{H}^{*}\times\boldsymbol{H}\right)}{4\omega}。 \tag{4}$$

2.2 光力和横向光力

光动量的变化会产生光力,光辐射压力是由光子被颗粒散射和吸收而产生的力,与光的散射方向有关。光辐射压力在原子冷却[2,36-38]、光学分选[39-42]、粒子推进等领域有重要应用。OGF 是由光场强度或相位分布不均匀而产生的力,与梯度方向有关。OGF 可以分为强度梯度力和相位梯度力,前者是由光场强度梯度而产生的力,它会吸引颗粒到达或排斥颗粒远离光场强度较大值的位置;而相位梯度力则是由光场相位梯度而产生的力,它会使物质沿着相位变化的方向运动。梯度力是光镊系统的基础,它在光学捕获[43-47]、生物探测、分选[45,48-54]、生物分子拉伸[55-58]和生物之间相互作用[59-63]等领域有广泛应用。在某种程度上,OGF 具有 OLF 的特征,却并不属于 OLF,因为 OLF 为垂直于波的传播方向且与光场梯度无关的力。因此,本文将仅对 OGF 简要介绍。根据 Rayleigh 近似,强度梯度力[1,64-66]可以表示为

$$\boldsymbol{F}_{\mathrm{grad}}=\frac{\mathrm{Re}(\alpha_{\mathrm{e}})}{4}\nabla|\boldsymbol{E}|^{2}=\frac{2\pi n_2 a^{3}}{c}\left(\frac{m_0^{2}-1}{m_0^{2}+2}\right)\nabla I, \tag{5}$$

式中:α_{e} 为颗粒的电极化率;a 为颗粒的半径;I 为光强;c 为真空中光速;$m_0=n_1/n_2$,n_1 和 n_2 分别为颗粒与介质的折射率。

关于相位梯度力,O'Neil 等[67]在 2002 年演示了颗粒沿拉盖尔-高斯光束的环形横断面运动,而该正式系统研究则由 Roichman 等[64]在 2008 年报道。对于振幅缓慢变化和相位空间变化的电场,在 t 时刻,$\boldsymbol{r}$ 处的电场矢量 $\boldsymbol{E}$ 可以表示为

$$\boldsymbol{E}(\boldsymbol{r},t)=E_0(\boldsymbol{r})\boldsymbol{u}_{\mathrm{pol}}\exp\left[\mathrm{i}\varphi(r)\right], \tag{6}$$

式中:$E_0(\boldsymbol{r})$ 为振幅;$\varphi(r)$ 则是快速变化的相位,r 为矢量 $\boldsymbol{r}$ 的模;$\boldsymbol{u}_{\mathrm{pol}}$ 为极化矢量。则相位梯度力[28,64,68]可以表示为

$$\boldsymbol{F}_{\mathrm{phase}}=\mathrm{Im}(\alpha_{\mathrm{e}})E_0^{2}\nabla\varphi/2。 \tag{7}$$

不难发现,这种相位梯度力的大小仅取决于粒子极化率相位梯度及强度,而与光强度梯度没有直接的关系。一般情况下,相位梯度力比强度梯度力要小许多。在特定的情况下,相位梯度力可以变得很突出,例如当 $\mathrm{Im}(\alpha_{\mathrm{e}})\gg\mathrm{Re}(\alpha_{\mathrm{e}})$[68]时,或者是在特别设计的相位快速变化、振幅缓慢变化的光场中。尽管相位梯度力也具备 OLF 的一些特征,即与波的传播方向垂直,但其仍不属于典型的 OLF[64,69-71],因为它与场相位梯度有关,本质上与 Poynting 动量有关,因此不再对相位梯度力作进一步讨论。

OLF 是一种垂直于光传播方向且与光场强度梯度和相位梯度无关的力。产生 OLF 的关键是打破系统的对称性,从而使光子在物质上施加横向动量。自 OLF 被发现以来,人们已经提出了很多不同的方法和机制来实现和探索 OLF,例如利用光的自旋和轨道动量[30,31,34,72-73]、CPL 和物体的手性耦合[74-77]、SOI[78-80]、SPP[81-83]等,如图 1 所示。实际上,无论是线性动量还是角动量都可以产生 OLF,且与 OLF 密切相关。如 BSM 或 SAM 都可以产生横向自旋力[84]。Nieto-Vesperinas 和 Xu[85]提出 IPM 也可以产生 OLF,这种 OLF 被称为 IPM 力。通过手性产生 OLF 也是人们研究的一个热点,Wang 和 Chan[74]提出了粒子手性可以在界面与散射波相耦合,产生横向的能量通量和力。Hayat 等[34]研究了手性粒子在具有横向 SAM 的倏逝波中受到的 OLF。Sukhov 等[78]通过观察条状圆偏振高斯光束照射聚苯乙烯粒子在空气和水界面产生的横向运动,发现由 SOI 作用可以产生 OLF。Rodríguez-

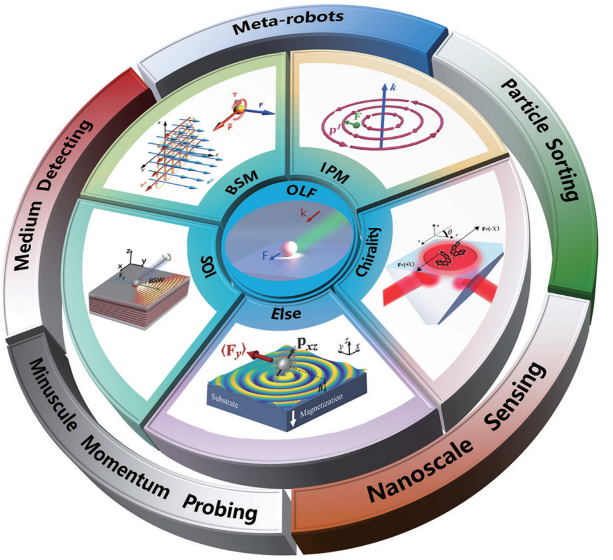

图 1　OLF 的不同分类和应用[30,32-35]

Fig. 1　Different classifications and applications of OLF[30,32-35]

Fortuño 等[79]通过使用 CPL 照射金表面附近的纳米颗粒，从理论上研究了 SPP 产生的 OLF。

3　产生横向光力的不同机制

3.1　由横向自旋动量产生的横向光力

对于金属[86]或高折射率电介质的磁介电颗粒[30,87-88]，由于横向 BSM 的存在，其 OLF 通常包含于场动量[30-31,85,88]中。这种 OLF 来源于电偶极子、磁偶极子、多极子间的干涉。偶极磁介电粒子所受光力[30,72,85,88-90]可以表示为

$$\boldsymbol{F}=\boldsymbol{F}_{\mathrm{e}}+\boldsymbol{F}_{\mathrm{m}}+\boldsymbol{F}_{\mathrm{em}},\tag{8}$$

式中：$\boldsymbol{F}_{\mathrm{e}}$、$\boldsymbol{F}_{\mathrm{m}}$、$\boldsymbol{F}_{\mathrm{em}}$ 分别为电偶极子、磁偶极子以及电磁偶极子相互作用所贡献的力。

电偶极子贡献的力 $\boldsymbol{F}_{\mathrm{e}}$[30,88-89]可具体表示为

$$\boldsymbol{F}_{\mathrm{e}}=\frac{1}{4}\mathrm{Re}\left(\alpha_{\mathrm{e}}\right)\nabla\left|\boldsymbol{E}\right|^{2}+\frac{2\omega}{\varepsilon}\mathrm{Im}\left(\alpha_{\mathrm{e}}\right)\boldsymbol{p}_{\mathrm{o,e}},\tag{9}$$

式中：$\boldsymbol{p}_{\mathrm{o,e}}$ 为轨道动量的电场部分。式(9)等号右侧的第一、第二项分别对应于场强度分布的电场部分以及电轨道动量密度的贡献(也称为辐射压力或散射力)。

与电偶极子贡献的部分类似，磁偶极子贡献的力 $\boldsymbol{F}_{\mathrm{m}}$[30,88-89]可以表示为

$$\boldsymbol{F}_{\mathrm{m}}=\mathrm{Re}\left(\alpha_{\mathrm{m}}\right)\nabla\left|\boldsymbol{B}\right|^{2}/4+2\omega\mu\mathrm{Im}\left(\alpha_{\mathrm{m}}\right)\boldsymbol{p}_{\mathrm{o,m}},\tag{10}$$

式中：$\boldsymbol{p}_{\mathrm{o,m}}$ 为轨道动量的磁场部分；α_{m} 为颗粒的复磁极化率。类似地，式(10)等号右侧的第一、第二项分别对应于场强度分布的磁场部分以及磁轨道动量密度的贡献。

电磁偶极子相互作用所贡献的力 $\boldsymbol{F}_{\mathrm{em}}$[88,91]可以表示为

$$\boldsymbol{F}_{\mathrm{em}}=-\frac{k^{4}}{12\pi}\sqrt{\frac{\mu}{\varepsilon}}\mathrm{Re}\left(\boldsymbol{d}\times\boldsymbol{m}^{*}\right)=$$
$$-\frac{\mu ck^{4}}{6\pi\varepsilon}\mathrm{Re}\left(\alpha_{\mathrm{e}}\alpha_{\mathrm{m}}^{*}\right)\left(\boldsymbol{p}_{\mathrm{s}}+\boldsymbol{p}_{\mathrm{o}}\right)+\frac{\mu ck^{4}}{6\pi\varepsilon}\mathrm{Im}\left(\alpha_{\mathrm{e}}\alpha_{\mathrm{m}}^{*}\right)\boldsymbol{p}_{\mathrm{I}},\tag{11}$$

式中：k 为光在介质中的波数；$\boldsymbol{d}$ 和 $\boldsymbol{m}$ 分别为电偶极矩和磁偶极矩。式(11)等号右侧第一项为时间平均 Poynting 动量的贡献，即 $\boldsymbol{p}=\mathrm{Re}\left(\boldsymbol{E}\times\boldsymbol{H}^{*}\right)/\left(2c^{2}\right)$，可写成 $\boldsymbol{p}=\boldsymbol{p}_{\mathrm{s}}+\boldsymbol{p}_{\mathrm{o}}$。而等号右侧第二项为来自 IPM 的力，即 $\boldsymbol{p}_{\mathrm{I}}=\mathrm{Im}\left(\boldsymbol{E}\times\boldsymbol{H}^{*}\right)/\left(2c^{2}\right)$。横向自旋动量 BSM（$\boldsymbol{p}_{\mathrm{s}}=\nabla/2\times\boldsymbol{S}$）可以产生一个来源于 SAM 不均匀性的力[72,92]。例如，聚焦的光束由于 SAM 不均匀可产生 OLF。电磁偶极子相互作用贡献的力 $\boldsymbol{F}_{\mathrm{em}}$ 由于包含小参量 ka 的更高次项，因此会比 $\boldsymbol{F}_{\mathrm{e}}$ 和 $\boldsymbol{F}_{\mathrm{m}}$ 小很多，导致 BSM 力也十分微弱，进而被梯度力与散射力所掩盖。除了梯度力与散射力外，式(11)等号右侧第一项中轨道动量部分也可能比 BSM 力大很多。值得一提的是，OLF 的方向与颗粒的材料属性有关[31,93-94]，

$$\mathrm{Re}\left(\alpha_{\mathrm{e}}\alpha_{\mathrm{m}}^{*}\right)\cong\frac{k^{2}a^{8}}{30}\left|\frac{\varepsilon_{\mathrm{p}}-\varepsilon}{\varepsilon_{\mathrm{p}}+2\varepsilon}\right|^{2}\left[\mathrm{Re}\left(\varepsilon_{\mathrm{p}}\right)+2\right],\tag{12}$$

式中：ε_{p} 为颗粒的介电常数。对于金纳米颗粒 $\mathrm{Re}\left(\varepsilon_{\mathrm{p}}\right)+2<0$；而对介电纳米颗粒，$\mathrm{Re}\left(\varepsilon_{\mathrm{p}}\right)+2>0$，这导致两种颗粒所受 OLF 的方向相反。关于 BSM 产生 OLF 的更多理论研究可参阅相关参考文献[30，93]。

图 2(a)左图展示了在右旋 CPL(R-CPL)以及左旋 CPL(L-CPL)光阱(聚焦在数值孔径 NA=1.2 上的高斯光束)中捕获的直径为 100 nm 的二氧化硅球上计算出的光力三维流线[95]，其展现出明显的螺旋轨迹。而实验测量的右旋 CPL 光阱对直径为 1 μm 的聚苯乙烯球施加的二维力场流线[图 2(a)右图]，进一步说明了自旋动量力可以对粒子产生旋转转矩。颗粒在聚焦 CPL 的高斯光束中的旋转示意图如图 2(b)所示。OLF 只存在于一个非平衡并且不稳定的位置[96]，因为强 OGF 会将粒子吸引到能够被稳定捕获的位置上，而该位置并不存在明显的横向力。

BSM 力的产生依赖于 SAM 的不均匀性，即椭圆偏振光场的非均匀分布会产生 BSM 力。因此，通过双波干涉的驻波来产生 OLF 是一种常见方法[91,97]，如图 2(b)和图 2(c)所示。然而利用双波干涉场产生 OLF 的方法存在一个巨大缺陷，粒子在三维空间中是自由扩散的，而每个点上的 OLF 大小可能都不一样，这会带来很大的不确定性。针对这种情况，人们引入了界面。但是界面也会产生额外的不确定因素，即 SOI 引起的光力，这种光力的作用可能会远大于 OLF，同样给 OLF 的观测和利用带来挑战。因此，需要用折射率匹配方法消除界面的影响。如图 2(d)所示，本研究团队利用与上下两片盖玻片折射率相同的液体，给颗粒提供了一个折射率均匀的环境，以减轻界

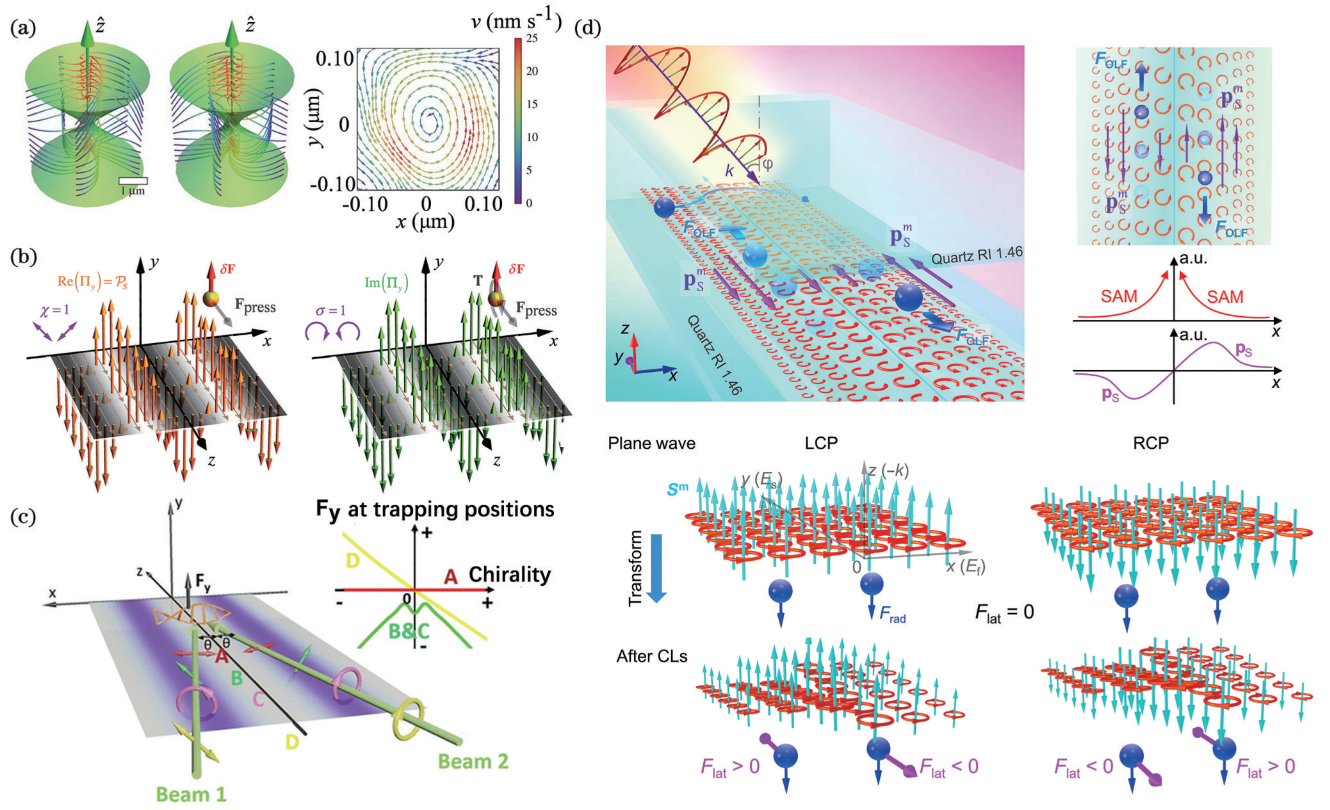

图 2 自由空间光波场中横向 BSM 产生的 OLF。(a)数值孔径为 1.2 的 R-CPL 和 L-CPL 以及直径为 100 nm 的二氧化硅粒子的力流线[95];(b)双光束干涉驻波场中源于横向 SAM 的 OLF[31];(c)通过干涉场中的可逆 OLF 实现全光学手性灵敏分选[97];(d)线状光场照射下聚苯乙烯颗粒上的 OLF[72]

Fig. 2 OLF generated by transverse BSM in free space optical wave field. (a) Force streamlines for using R-CPL and L-CPL with numerical aperture of 1.2 and silicon dioxide particles with diameter of 100 nm[95]; (b) OLF from transverse SAM in double beam interference standing wave field[31]; (c) all-optical chiral-sensitive realized by reversible OLF in interference field[97]; (d) OLF on polystyrene particles under linear light field illumination[72]

面上强 SOI 效应的影响,也为 OLF 的探测提供了一个均匀的环境[72]。特别是利用单束线状光场时,可以大大削弱横向 OGF 的影响,这也演示了从非均匀自旋场中获得稳定双向 OLF 的普遍现象。研究表明,该 OLF 的振幅和方向取决于光束的椭偏度。

为了减轻横向 OGF 对 OLF 研究的干扰,Bliokh 等[30]研究了由全内反射产生的单色倏逝波的横向自旋和 OLF,如图 3(a)所示。这样的光场会产生一个衰减的 OGF,将颗粒吸附在全内反射界面上,这给 OLF 的研究提供了一个理想平台[34]。横向自旋相关 OLF 的大小和方向与全内反射入射波的横电(TE)模和横磁(TM)模分量的比例密切相关,无论是线性偏振还是椭圆偏振,均可由相应的归一化 Stokes 参数描述,具体表达式为

$$\begin{cases}\tau=\left(1-|m|^{2}\right)/\left(1+|m|^{2}\right)\\ \chi=\left[2\mathrm{Re}(m)\right]/\left(1+|m|^{2}\right),\\ \sigma=\left[2\mathrm{Im}(m)\right]/\left(1+|m|^{2}\right)\end{cases}\tag{13}$$

式中:τ 为庞加莱球上水平或垂直方向的偏振程度,即线偏振的方向;χ 为实螺旋度;σ 为螺旋度,$\sigma=\pm1(\pm\mathrm{i})$ 对应了线性对角或反对角极化(左旋或右旋);参数 m 决定了偏振[30,85]。

沿 z 方向传播并沿 x 轴衰减的倏逝波的横向自旋时间平均 Poynting 动量[30,85]可以表示为

$$p_{s,y}=p_y\propto\sigma\left(\frac{\kappa_0 k}{k_z}\right)w,\tag{14}$$

式中:p_y 为时间平均 Poynting 动量的横向分量,为复数;κ_0 为指数衰减率;k_z 为纵波数;w 为能量密度。

显而易见的是,Poynting 动量的横向分量完全来源于 BSM 的横向分量,而横向 IPM[30,85]可以表示为

$$\mathrm{Im}\left(p_y\right)\propto-\chi\left(\frac{\kappa k}{k_z}\right)w,\tag{15}$$

值得强调的是,$\mathrm{Im}\left(p_y\right)$ 同样完全来源于自旋动量虚部的横向部分。Nieto-Vesperinas 和 Xu 将磁介电粒子置于倏逝波场中,建立了能够区分来源于 $\mathrm{Im}\left(p_y\right)$ 或 p_y 的 OLF,可以说明 $\mathrm{Im}\left(p_y\right)$ 完全来源于横向自旋动量虚部 $\mathrm{Im}\left(p_{s,y}\right)$,而垂直于界面的动量虚部 $\mathrm{Im}\left(p_z\right)$ 则完全来

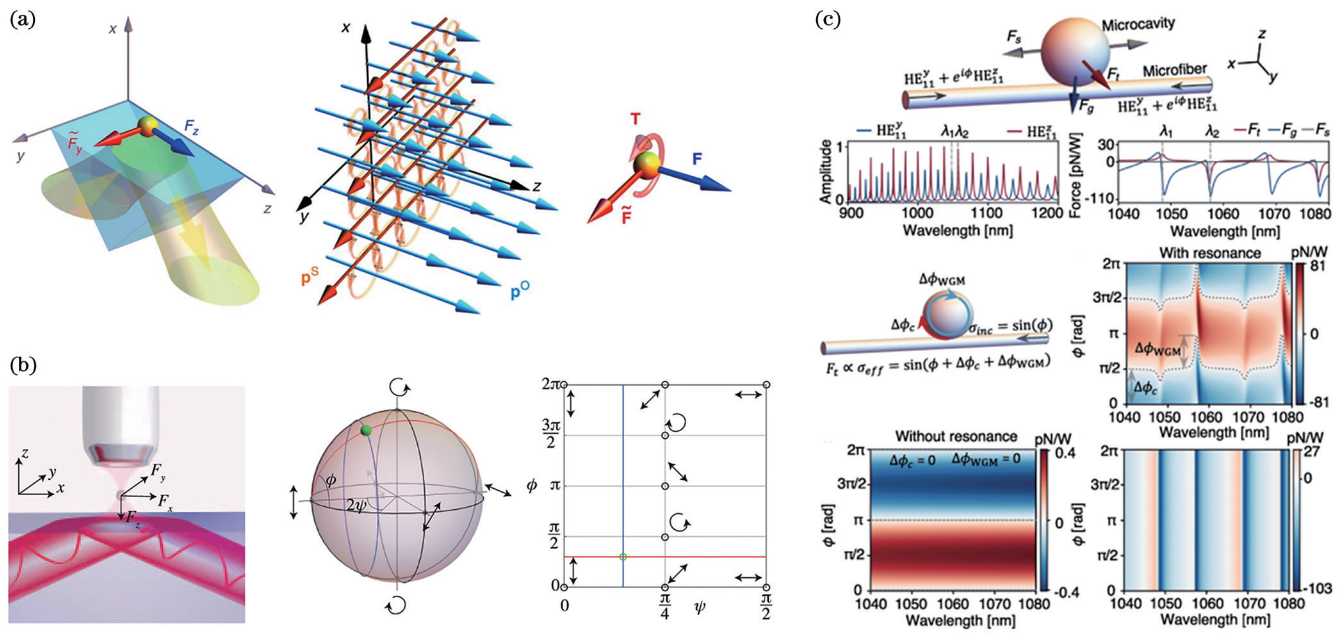

图3 近场横向BSM产生的OLF。(a)倏逝波中横向BSM产生的OLF[30];(b)庞加莱球面上具有不同极化程度倏逝波中的OLF[98];(c)微纤维-微腔系统中的OLF[100]

Fig. 3 OLF generated by transverse BSM in near field. (a) OLF generated by transverse BSM in evanescent waves[30]; (b) OLF in evanescent waves with different degrees of polarization on Poincaré sphere[98]; (c) OLF from microfiber-microcavity system[100]

源于 $\mathrm{Im}(p_{s,z})$。这种效应使得 $\mathrm{Im}(p_{s,y})$、$\mathrm{Im}(p_y)$、$\mathrm{Im}(p_z)$、$\mathrm{Im}(p_{s,z})$均可被观测[84]。

Ginis等[98]发现当光束有对角极化时,OLF的最大值并非对应着L-CPL或R-CPL,这说明来源于BSM的OLF的最大值通常出现在L-CPL或R-CPL的结论[30,31,99]是不正确的。由图3(b)可知,通过研究庞加莱球中的方向角与椭圆度角,可以发现最大或者最小的OLF并不一定对应球体上北极或南极的圆偏振。最近,Lu等[100]发现当一个粒子被放置在微纤维-微腔系统中时,一个额外的螺旋度项有助于OLF的产生,即使光的螺旋度为零,也可能会产生一个OLF,如图3(c)所示。

2016年,Antognozzi等[99]报道了利用横向BSM产生OLF的实验。如图4(a)所示,当探针粒子被置于全内反射界面附近时,纳米悬臂梁可用于测量倏逝波中的OLF。2018年,Liu等[101]报道了来自BSM和横向自旋光力的三维测量技术并作用在米氏(Mie)粒子上,如图4(b)所示。实验开发了一种利用扫描功能来绘制粒子与光波之间相互作用体积图的新方法,并实现了fN数量级的分辨率。这种方法为人们系统研究奇异光力提供了一种新手段。

虽然BSM力的概念源于偶极子模型[88],但最近被推广到更为一般的任意阶多极子模型[102]。在圆偏振环形光束中,这种高阶BSM力在方位角方向上产生,并且与局部相位梯度和强度梯度都正交。

SOI是一种影响OLF的重要因素,它描述了光的自旋动量和轨道动量之间的耦合。如前文所述,本研究团队[72]将聚苯乙烯颗粒置于石英玻片中,该石英片与聚乙二醇有着相同的折射率,能够减轻界面的影响,并且将激光束聚焦为线状光场,这一操作可以有效减少横向OGF的影响,为研究自旋动量诱导的OLF提供了良好的环境,实验示意图如图4(c)所示。最近,Stilgoe[103]将两束自旋相反的光束结合在一起并产生非零横向SAM,这种SAM可以转移到双折射球霰石微粒上,并使其沿着不同平面上的轨道运行,如图4(d)所示。

综上所述,BSM力通常不是直接来自SAM,而是来自它的旋度。Yu等[104]从理论上获得了一种存在于倏逝波中异常的OLF,并与SAM成正比。这似乎与之前的研究结果相矛盾,即OLF只能由IPM或BSM(后者是SAM的旋度)产生[30,85]。这是因为在纯横向自旋的特定条件下,$\mathrm{Im}(p^*\cdot q)=0$,并且横向IPM与SAM互成比例,即 $P_{\mathrm{I,trans}}\propto \mathrm{Re}(p^*\cdot q)S_{\mathrm{trans}}$(其中,$P_{\mathrm{I,trans}}$、$S_{\mathrm{trans}}$分别为横向IPM和横向SAM的大小,$p$、$q$为极化参数且满足$|p|^2+|q|^2=1$,$p^*$为$p$的共轭,详见参考文献[104])。然而,在一般情况下,非手性球形颗粒上的光力与自旋无关[86],但其手性颗粒上的光力方向可以直接平行于SAM。

3.2 手性颗粒上的横向光力

手性颗粒在电磁波中的本构关系[75,105-106]可表示为

$$\boldsymbol{D}=\varepsilon_{\mathrm{p}}\boldsymbol{E}+\mathrm{i}\kappa\sqrt{\varepsilon_0\mu_0}\,\boldsymbol{H},\tag{16}$$

$$\boldsymbol{B}=-\mathrm{i}\kappa\sqrt{\varepsilon_0\mu_0}\,\boldsymbol{E}+\mu_{\mathrm{p}}\boldsymbol{H},\tag{17}$$

式中:$\boldsymbol{D}$和$\boldsymbol{B}$分别为电位移矢量和磁感应强度;ε_0和μ_0

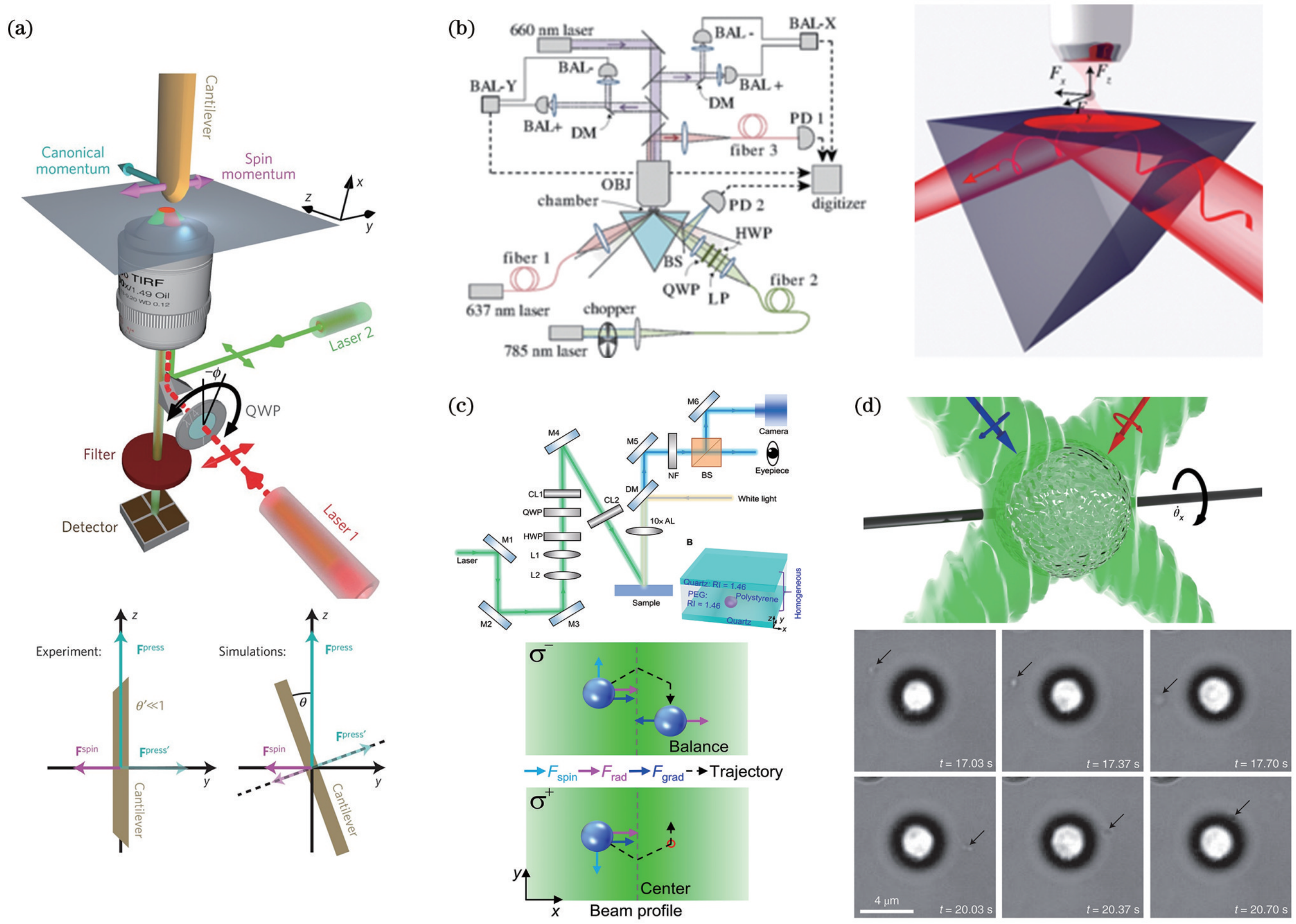

图 4　有关来自横向BSM的OLF的实验和研究。(a)纳米机械悬臂测量[99]；(b)Mie颗粒上横向自旋力三维测量装置[101]；(c)在均匀环境中产生线状光场以实现粒子上稳定的OLF的实验示意图[72]；(d)小粒子被驱动着围绕大颗粒进行横向旋转[103]

Fig. 4　Experiments and research on OLF from transverse BSM. (a) Nanomechanical cantilever measurements[99]; (b) three-dimensional measurement setup for transverse spin force on Mie particle[101]; (c) experimental schematic for generating line-shaped light field in uniform environment to achieve stable OLF on particle[72]; (d) small particle driven to rotate laterally around larger particle[103]

分别为真空中的介电常数和磁导率；μ_{p} 为颗粒的磁导率；κ 为手性参数并且满足 $\kappa<\sqrt{\varepsilon\mu}$[107-108]。

手性颗粒中诱导的电磁偶极矩与入射场 $\boldsymbol{E}$、$\boldsymbol{B}$ 关系[74,91,97,109]可表示为

$$\boldsymbol{d}=\alpha_{\mathrm{ee}}\boldsymbol{E}+\alpha_{\mathrm{em}}\boldsymbol{B},\tag{18}$$

$$\boldsymbol{m}=-\alpha_{\mathrm{em}}\boldsymbol{E}+\alpha_{\mathrm{mm}}\boldsymbol{B},\tag{19}$$

式中：α_{ee}、α_{em}、α_{mm} 为颗粒的极化率，α_{em} 与手性参数 κ 有关，并随 κ 变化改变其符号。对于非手性颗粒，$\alpha_{\mathrm{em}}=0$。极化率 α_{ee}、α_{em}、α_{mm} 与 Mie 系数 $a_1^{(1)}$、$b_1^{(1)}$、$a_1^{(2)}$ 的关系可表示为

$$\begin{cases}\alpha_{\mathrm{ee}}=\mathrm{i}6\pi\varepsilon a_1^{(1)}/k^3\\ \alpha_{\mathrm{mm}}=\mathrm{i}6\pi b_1^{(1)}/\left(\mu k^3\right)\\ \alpha_{\mathrm{em}}=-6\pi a_1^{(2)}/\left(Z_0k^3\right)\end{cases},\tag{20}$$

式中：$Z_0=\sqrt{\mu/\varepsilon}$ 为介质中的波的阻抗。光力公式为

$$\boldsymbol{F}=\frac{1}{2}\mathrm{Re}\left[\boldsymbol{d}\cdot(\nabla)\boldsymbol{E}^*+\boldsymbol{m}\cdot(\nabla)\boldsymbol{B}^*-\frac{k^4}{6\pi\varepsilon c}\boldsymbol{d}\times\boldsymbol{m}^*\right]。\tag{21}$$

将式(20)代入，可以得到手性颗粒上的光力表达式[91,110]，具体计算过程为

$$\boldsymbol{F}=\boldsymbol{F}_{\mathrm{grad}}+\boldsymbol{F}_{\mathrm{rad}}+\boldsymbol{F}_{\mathrm{curl}}+\boldsymbol{F}_{\mathrm{spin}}+\boldsymbol{F}_{\mathrm{IPM}},\tag{22}$$

其中，

$$\boldsymbol{F}_{\mathrm{grad}}=-\nabla U,\tag{23}$$

$$\boldsymbol{F}_{\mathrm{rad}}=\left(\sigma_{\mathrm{ext}}+\sigma_{\mathrm{recoil}}\right)\boldsymbol{P}/c,\tag{24}$$

$$\boldsymbol{F}_{\mathrm{curl}}=\sigma_{\mathrm{e}}c\left(\nabla\times\boldsymbol{S}_{\mathrm{e}}\right)+\sigma_{\mathrm{m}}c\left(\nabla\times\boldsymbol{S}_{\mathrm{m}}\right)+\mu\mathrm{Re}\left(\alpha_{\mathrm{em}}\right)\left(\nabla\times\boldsymbol{P}\right),\tag{25}$$

$$\boldsymbol{F}_{\mathrm{spin}}=\left[2\omega^2\mu\mathrm{Re}\left(\alpha_{\mathrm{em}}\right)-\frac{k^5}{3\pi\varepsilon^2}\mathrm{Im}\left(\alpha_{\mathrm{ee}}\alpha_{\mathrm{em}}^*\right)\right]\boldsymbol{S}_{\mathrm{e}}+\left[2\omega^2\mu\mathrm{Re}\left(\alpha_{\mathrm{em}}\right)-\frac{k^5\mu}{3\pi\varepsilon}\mathrm{Im}\left(\alpha_{\mathrm{mm}}\alpha_{\mathrm{em}}^*\right)\right]\boldsymbol{S}_{\mathrm{m}},\tag{26}$$

$$\boldsymbol{F}_{\mathrm{IPM}}=\frac{ck^4\mu^2}{12\pi}\mathrm{Im}\left(\alpha_{\mathrm{ee}}\alpha_{\mathrm{em}}^*\right)\mathrm{Im}\left(\boldsymbol{E}\times\boldsymbol{H}^*\right),\tag{27}$$

式中：$\boldsymbol{F}_{\mathrm{grad}}$ 为光强度梯度力，其中电势 $U=-\mathrm{Re}\left(\alpha_{\mathrm{ee}}\right)|\boldsymbol{E}|^2/4-\mathrm{Re}\left(\alpha_{\mathrm{mm}}\right)|\boldsymbol{B}|^2/4+\mathrm{Re}\left(\alpha_{\mathrm{em}}\right)\times\mathrm{Im}\left(\boldsymbol{B}\cdot\boldsymbol{E}^*\right)/2$；$\boldsymbol{F}_{\mathrm{rad}}$ 为与时间平均 Poynting 动量

$\left[\boldsymbol{P}=\mathrm{Re}\left(\boldsymbol{E}\times\boldsymbol{H}^{*}\right)/2\right]$成比例的光辐射压力，其中$\sigma_{\mathrm{ext}}$为电、磁偶极子总的消光截面，$\sigma_{\mathrm{e}}$和$\sigma_{\mathrm{m}}$分别为电偶极子的消光截面和磁偶极子的消光截面，$\sigma_{\mathrm{ext}}=\sigma_{\mathrm{e}}+\sigma_{\mathrm{m}}=k\mathrm{Im}\left(\alpha_{\mathrm{ee}}\right)/\varepsilon+k\mu\mathrm{Im}\left(\alpha_{\mathrm{mm}}\right)$，$\sigma_{\mathrm{recoil}}$为与反冲力相关的消光截面，$\sigma_{\mathrm{recoil}}=-\frac{k^{4}\mu}{6\pi\varepsilon}\left[\mathrm{Re}\left(\alpha_{\mathrm{ee}}\alpha_{\mathrm{em}}^{*}\right)+\left|\alpha_{\mathrm{em}}\right|^{2}\right]$[11]；$\boldsymbol{F}_{\mathrm{curl}}$为自旋动量产生的力，即BSM力；$\boldsymbol{F}_{\mathrm{spin}}$为自旋力，表示仅来源于手性颗粒与SAM密度的耦合产生的力，而非手性颗粒没有这种力，$\boldsymbol{S}_{\mathrm{e}}$和$\boldsymbol{S}_{\mathrm{m}}$分别为电自旋角动量密度和磁自旋角动量密度；$\boldsymbol{F}_{\mathrm{IPM}}$与IPM相关[85]，也与粒子周围和内部存储能量的交替流动相关，当颗粒为磁电颗粒时，这种力极为重要[88,110]。另一方面，对于平面波或者倏逝波中的非磁电颗粒，$\boldsymbol{F}_{\mathrm{grad}}$、$\boldsymbol{F}_{\mathrm{rad}}$、$\boldsymbol{F}_{\mathrm{curl}}$、$\boldsymbol{F}_{\mathrm{IPM}}$是可以忽略的，而$\boldsymbol{F}_{\mathrm{spin}}$比$\boldsymbol{F}_{\mathrm{vor}}$（能流旋度产生的力）要小很多。因此，想要估计手性颗粒与光耦合产生的OLF，分析Poynting动量的横向分量是一种有效的途径[75]。

图5展示了单光束光阱中手性颗粒的光力。由图5(a)可知，在螺旋度$\Lambda>0$或者$\Lambda<0$的椭圆偏振中，手性参数$\kappa>0$的手性球形颗粒会在光阱中被捕获或排斥。这种机制使得手性颗粒可以被困在光束的焦点或空心光束中[111-114]。而Yamanishi等[115]发现手性颗粒的共振对光场的扰动也会对OGF产生显著的影响。为了验证这种效应，通过合成不同共振特性的金颗粒，展示了依赖光场螺旋性并且与手性颗粒共振相关的OGF，相关实验现象如图5(b)所示。最近，Cipparrone等[112]通过切换光偏振，实现了捕获、排斥手性胆甾相液晶粒子，相关实验现象如图5(c)所示。这项研究将为手性颗粒光力的研究提供新的思路，并由此产生传感与分选相关的新方法。

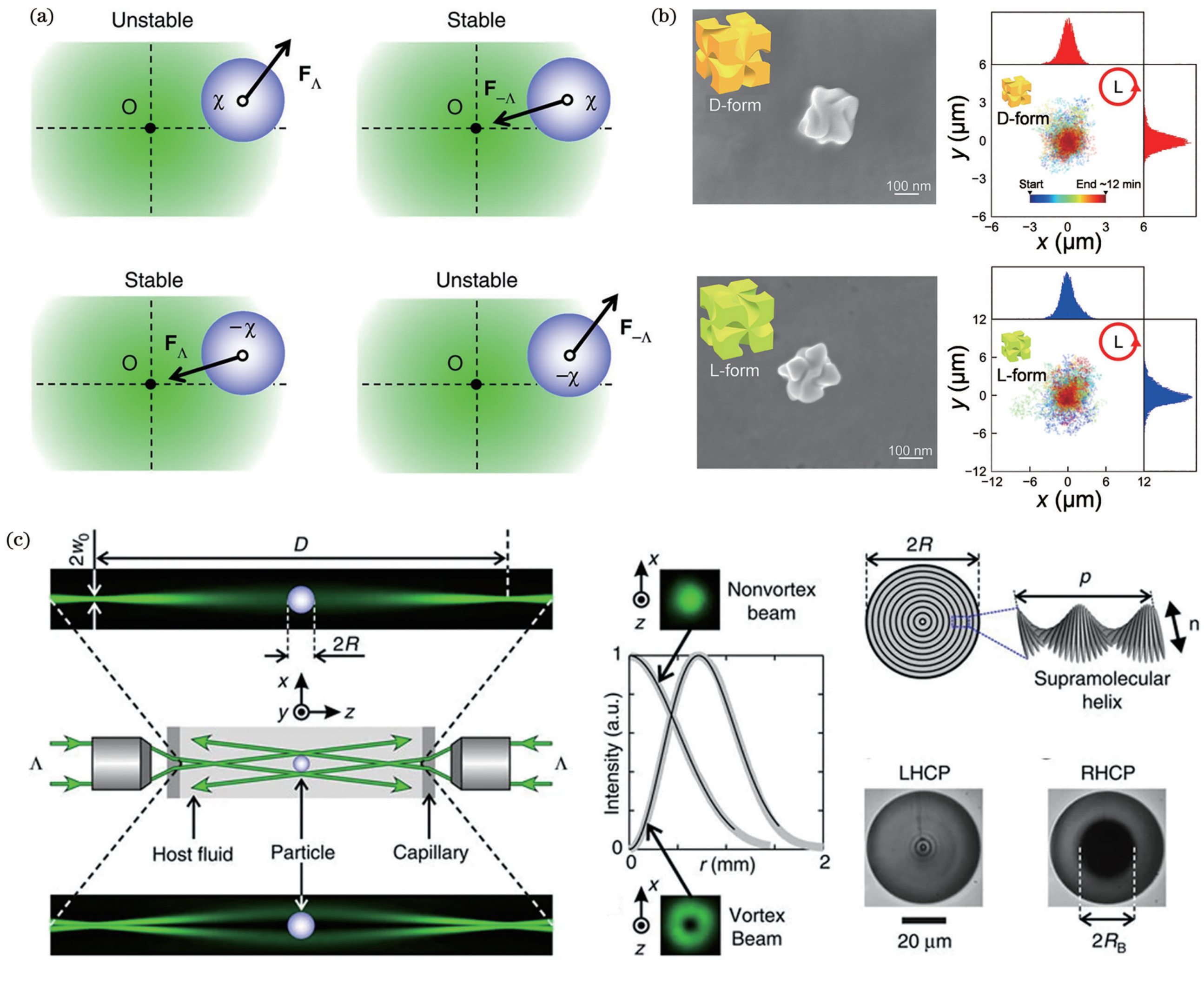

图5　手性颗粒上的OGF。(a)手性颗粒的三位捕获示意图[111]；(b)手性金纳米颗粒的扫描电镜图像以及手性金纳米颗粒捕获实验示意图[115]；(c)径向各向同性手性微球的光学捕获和排斥[112]

Fig. 5　OGF on chiral particles. (a) Illustration of three-dimensional capture of chiral particles[111]; (b) scanning electron microscope images of chiral gold nanoparticles and schematic diagram of chiral gold nanoparticle capture experiment[115]; (c) optical capture and repulsion of radial isotropic chiral microspheres[112]

虽然OGF能够运用于手性颗粒分选，但是布朗运动会对其运动观测产生干扰，并且OGF自身效率较低。相较而言，利用界面上或界面附近颗粒所受OLF来分选手性粒子，是一种更具可行性的双向对映体选择性分离方法。

当一束线偏振光照射处于界面上的手性颗粒时，手性与界面不对称会耦合产生OLF[74-75]，如图6(a)所示。这种OLF主要源于Poynting动量的不对称分布，即式(22)中的$\boldsymbol{F}_{\mathrm{rad}}$。同时，由衬底反射而引起的自旋力$\boldsymbol{F}_{\mathrm{spin}}$对其也有贡献。另一个方案便是利用线偏振倏逝波在手性颗粒上产生OLF，由倏逝场横向SAM密度与粒子的手性电磁响应直接相互作用而产生OLF，如图6(b)所示。因为在这种情况下既不存在横向场梯度，也不存在横向波的传播。由于光存在量子自旋霍尔效应[116-119]，一个固有的横向SAM被锁定在SPP的传播方向上，这种效应被称为自旋动量锁定[81,120-123]。横向SAM产生的OLF可以被解释为式(22)中的$\boldsymbol{F}_{\mathrm{spin}}$，这种情况下的自旋力$\boldsymbol{F}_{\mathrm{spin}}$甚至可能比光辐射压力$\boldsymbol{F}_{\mathrm{rad}}$大得多，因此OLF也比图6(a)中的大。来自横向SAM的OLF也可以在纳米探针[124]、光纤附近[125-126]以及贝塞尔光束[114]中找到。本研究团队[75]将不同手性的聚合液晶微粒放置在空气和水界面上，利用条状线偏振光照射，观测到了颗粒上的OLF，如图6(c)所示。同时，可以发现OLF的符号与粒子的大小、手性、入射光的入射角和偏振密切相关。Chen等[127]也用线偏振光在成对的不同手性颗粒上得到了方向相反的OLF，如图6(d)所示。

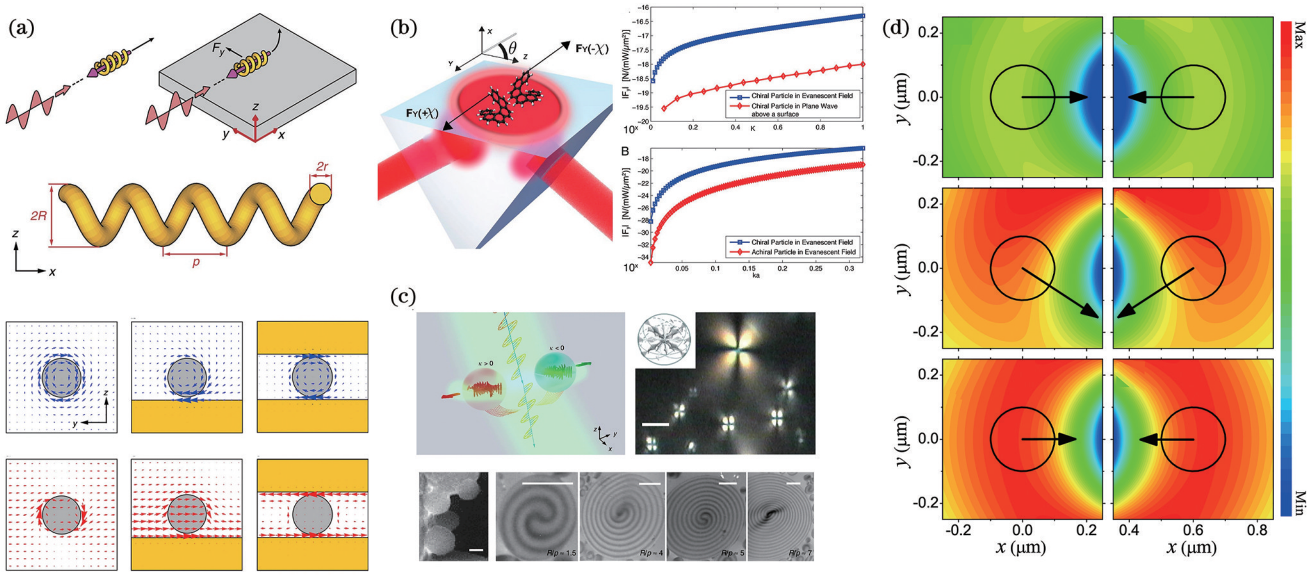

图6 线偏振光激发手性颗粒上的OLF。(a)通过手性与线偏振光的耦合对处于界面上的颗粒施加OLF[74]；(b)线偏振倏逝波中手性颗粒上的OLF[34]；(c)条状线偏振光产生可逆OLF[75]；(d)线偏振光在手性二聚体上产生OLF[127]

Fig. 6 Linearly polarized light excites OLF on chiral particle. (a) Applying OLF to particle at interface through coupling of chirality and linearly polarized light[74]; (b) OLF on chiral particle in linearly polarized evanescent wave[34]; (c) reversible OLF generated by line-shaped linearly polarized beam[75]; (d) linearly polarized light generates OLF on chiral dimers[127]

除了利用单一线偏光场，OLF也可能出现在例如驻波、涡旋光场等复杂光场中。Chen等[91]将手性颗粒放在双波干涉场中，所产生的OLF可推动手性颗粒，如图7(a)所示。这种OLF主要来自于光的涡旋度与粒子手性的耦合，即$\boldsymbol{F}_{\mathrm{curl}}$中的$\nabla\times\boldsymbol{P}$这一项。当手性参数$\kappa$较大时，它的数值可与光辐射压力$\boldsymbol{F}_{\mathrm{rad}}$和OGF相当。Zhang等[97]通过利用线形光场与CPL的干涉效应，发现了在两个平面波干涉场中的手性颗粒也有OLF。尽管可以通过不同的手性参数和光偏振来调整OLF的大小，但粒子的运动方向仍然保持不变，这使得分离该手性粒子变得十分困难。为了解决这一分选问题，本研究团队将纳米颗粒的一半浸入水中，另一半依旧暴露在空气中，利用线偏振光对不同纳米手性颗粒进行定向分选。Liu等[128]利用紧聚焦矢量偏振空心光束诱导的光力和扭矩来分离手性对映体，如图7(b)所示。最近，Li等[129]提出了一种利用紧聚焦矢量光束来分选手性颗粒的机制，如图7(c)所示。矢量光束中的径向OLF可以根据不同的手性参数捕获、排斥手性颗粒[128-130]。方位角方向的OLF源于颗粒SAM向OAM的转换，并与手性参数的虚部密切相关[129,131]。

利用光学Stern-Gerlach方法[132-133]，Kravets等[134]展示了不同手性粒子的双向分选，如图7(d)所示。在聚焦CPL高斯或拉盖尔-高斯光束中，以及在光场螺旋度和物质手性的相互作用下，可以选择性地捕获不同的手性液晶微球，这为利用手性光操控手性物体提供了一种新方法[111]。

手性相关的OLF与颗粒的手性极化率息息相关。颗粒的手性极化率通常比电极化率小很多，进一步导

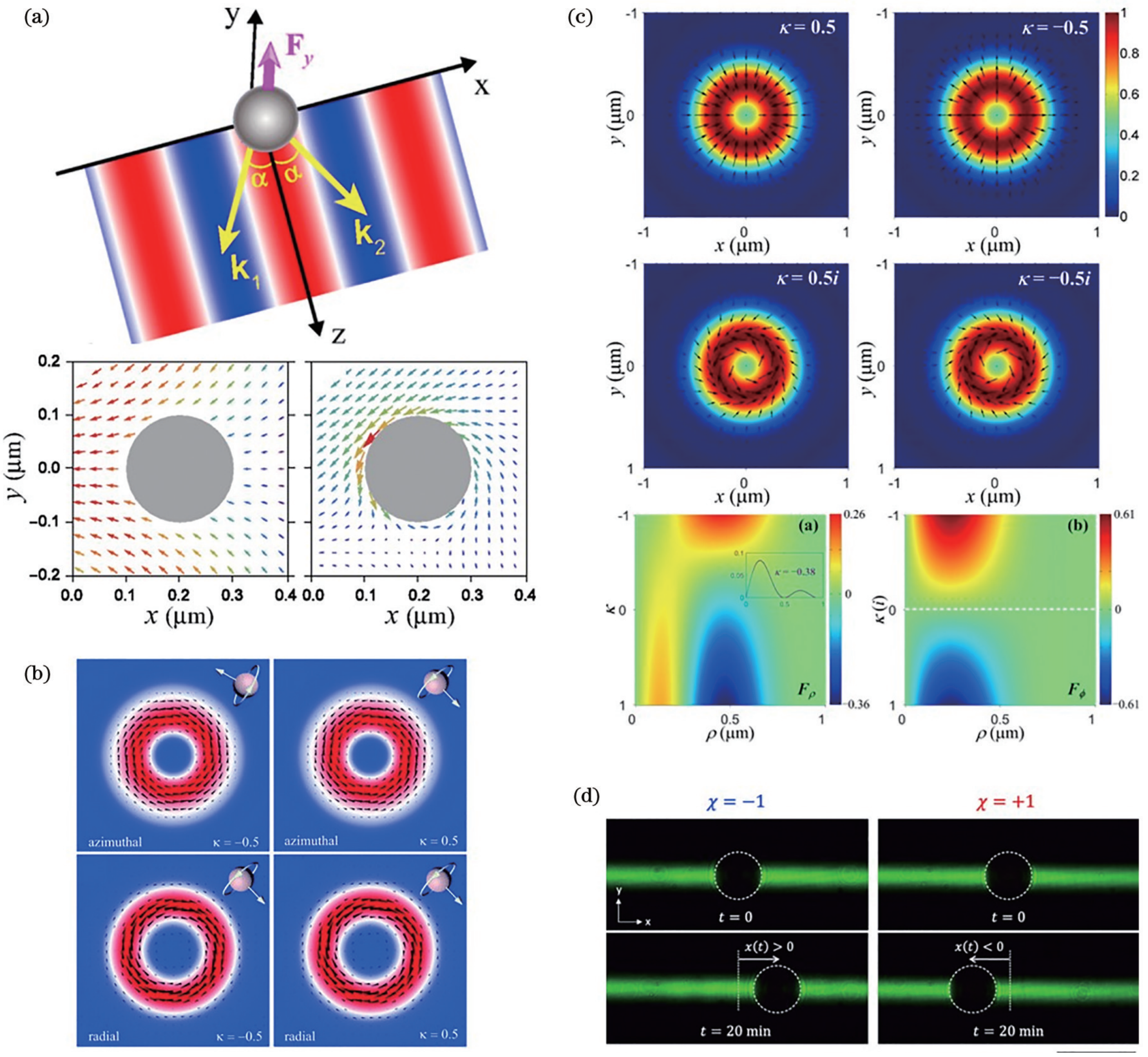

图 7　特殊光波中手性颗粒的 OLF。(a)手性粒子在双平面波干涉场中产生的 OLF 示意图[91]；(b)利用紧聚焦矢量偏振空心光束诱导的光力和扭矩分离手性对映体[128]；(c)手性颗粒在聚焦矢量光场中的 OLF 示意图以及 OLF 与颗粒手性参数和半径的函数示意图[129]；(d)利用手性液晶微球进行光学 Stern-Gerlach 牛顿实验[134]

Fig. 7　OLF on chiral particle in special light wave. (a) Schematic diagram of OLF generated by chiral particle in dual-plane wave interference field[91]; (b) separation of chiral enantiomers using optical force and torque induced by tightly focused vector-polarized hollow beam[128]; (c) schematic diagrams of OLF on chiral particle in a focused vector light field, and function of OLF with particle chirality parameters and radius[129]; (d) optical Stern-Gerlach Newton experiment using chiral liquid crystal microsphere[134]

致 OLF 比 OGF 或光辐射压力小很多。微弱的 OLF 使得其在传感和光学操控方面的广泛应用变得困难。因此，迫切需要增强手性相关的 OLF。

在手性环境中生成一个手性 SPP，从而能够产生一个手性敏感的强 OLF 来探测和分选手性粒子，如图 8(a)所示。手性 SPP 的 OLF 可能是由等离子体横向 SAM 转移为横向线性动量而产生的[135-136]，这种 OLF 在对映体分选和传感方面均具有巨大潜力。

除了偶极状态，多极分析虽然揭示了多极效应对角到线性交叉动量转移的影响，但这也会导致 OLF 在较大的手性粒子上发生符号反转，因此多级分析能够作为计算 Mie 手性粒子上增强光力的重要工具[135]。Cao 等[137]报道了在等离子体纳米孔径中使用 Fano 共振可以增强手性梯度力，使其超过非手性力，如图 8(b)所示。Fano 共振增强了手性密度力分量的梯度，从而增加了 OLF[138]，能够应用于手性对映体的分选。特殊的多极模态也可以增强 OLF，如 Zhu 等[76]研究了单手性纳米结构中多极的叠加效应，如图 8(c)所示。两个环向偶极子或电磁六极子可以组合形成一个混合模式，从而显著提高 OLF，使其达到与传统光辐射压力相同的量级。此外，两种模式也可以相互干扰和抵消，可产生一个连续体束缚态(BIC)，进而抑制定向散射并减少 OLF。

为了加强、控制和量化与光螺旋度相关的手性光力，Zhao 等[139]开发了一种手性原子力显微镜探针和等

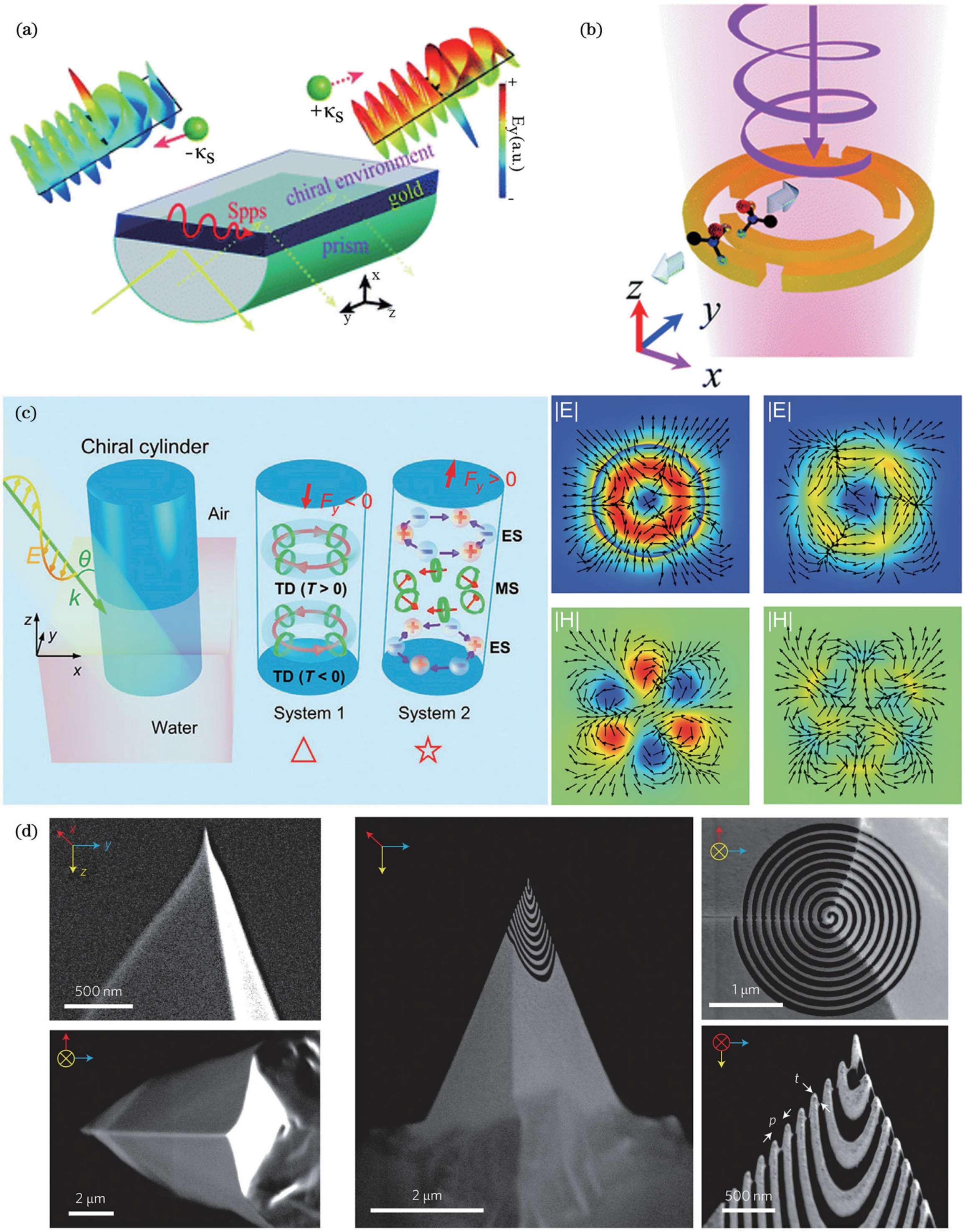

图 8　利用手性增强 OLF。(a)SPP 辅佐的手性对映体识别和分离的金属-手性 Kretschmann 构型的示意图[81]；(b)在金分裂环谐振器中通过 Fano 共振增强手性纳米粒子上的 OLF[137]；(c)单手性纳米结构中多极的叠加效应[76]；(d)非手性和手性显微镜探针的对映选择性光学力[139]

Fig. 8　Enhancing OLF using chirality. (a) Schematic diagram of metal-chiral Kretschmann configuration with SPP-assisted chiral enantiomer recognition and separation[81]; (b) enhancement of OLF on chiral nanoparticle through Fano resonance in gold split-ring resonator[137]; (c) multipole superposition effect in single chiral nanostructure[76]; (d) enantiomer-selective optical force using achiral and chiral microscope probes[139]

离子体光镊相结合的技术，如图 8(d)所示。用 CPL 照明等离子体光镊会对显微镜尖端施加一个力，该力的性质取决于光和尖端的旋向性。对于左手手性尖端，L-CPL 产生的横向力有吸引作用，而 R-CPL 产生的横向力具有排斥作用。利用核壳颗粒[140]或槽波导[141]也能增强光力或增加光力矩。

3.3 虚 Poynting 动量产生的横向光力

IPM 是一种描述光场中能量流动方向且与 Poynting 动量不一致的量，它可以在各种结构光场（如倏逝平面波和干涉场）中指向横向。IPM 力是由 IPM 与颗粒的相互作用而产生的。本节将介绍产生 IPM 相关的 OLF 的一些代表性方法和机制。

式（22）中的最后一项说明光力也可能来源于 IPM（$\boldsymbol{p}_{\mathrm{I}}$），偶极子的 IPM 力[85,88]可以表示为

$$\boldsymbol{F}_{\mathrm{IPM}}=\frac{\mu c k^4}{6\pi\varepsilon}\mathrm{Im}\left(\alpha_{\mathrm{e}}\alpha_{\mathrm{m}}^{*}\right)\boldsymbol{p}_{\mathrm{I}}。\tag{28}$$

IPM 力需要打破系统的电磁对称性（当 $\alpha_{\mathrm{e}}=\alpha_{\mathrm{m}}$ 时，$\boldsymbol{F}_{\mathrm{IPM}}=0$），但是物质通常具有双不对称性，因为存在电荷但并不存在磁荷。事实上，IPM 力的理论可以推广到偶极子近似之外，具体表达式[86]为

$$\boldsymbol{F}_{\mathrm{IPM},N}=\sum_{l=1}^{N}2c^2A_{N,l}\left(k^2+\frac{\Delta}{2}\right)^{l-1}\boldsymbol{p}_{\mathrm{I}},\tag{29}$$

式中：正整数 N 表示所包含的多极子的最高阶数；系数 $A_{N,l}$ 由粒子性质决定；Δ 为拉普拉斯算子。

在实验中想要观察到横向 IPM 力是具有挑战性的[142]，类平面波的功率密度相当有限，IPM 力也是如此。虽然使用纳米悬杆可以显著增加 IPM 力的大小[99]，但是棒状探针的高度各向异性特性同时会产生光学转矩[143-144]，这会阻碍对 IPM 力的单独观察。

为了检测 IPM 力，Xu 和 Nieto-Vesperinas[32]提出了一种矢量光束，在此光场中，自旋动量消失，而 IPM 呈涡旋结构并横向于局部轨道动量和强度梯度，如图 9（a）所示。此外，该场的环状强度轮廓允许光学捕获在 IPM 非零的非轴位置。Zhou 等[86]利用 IPM 涡旋束和各向同性金属微探针观察到横向 IPM 力，实验装置如图 9（b）所示。球体围绕束轴双向旋转，这种旋转不依赖于光学自旋和 OAM，可为光学扳手提供一种替代方法[145]。

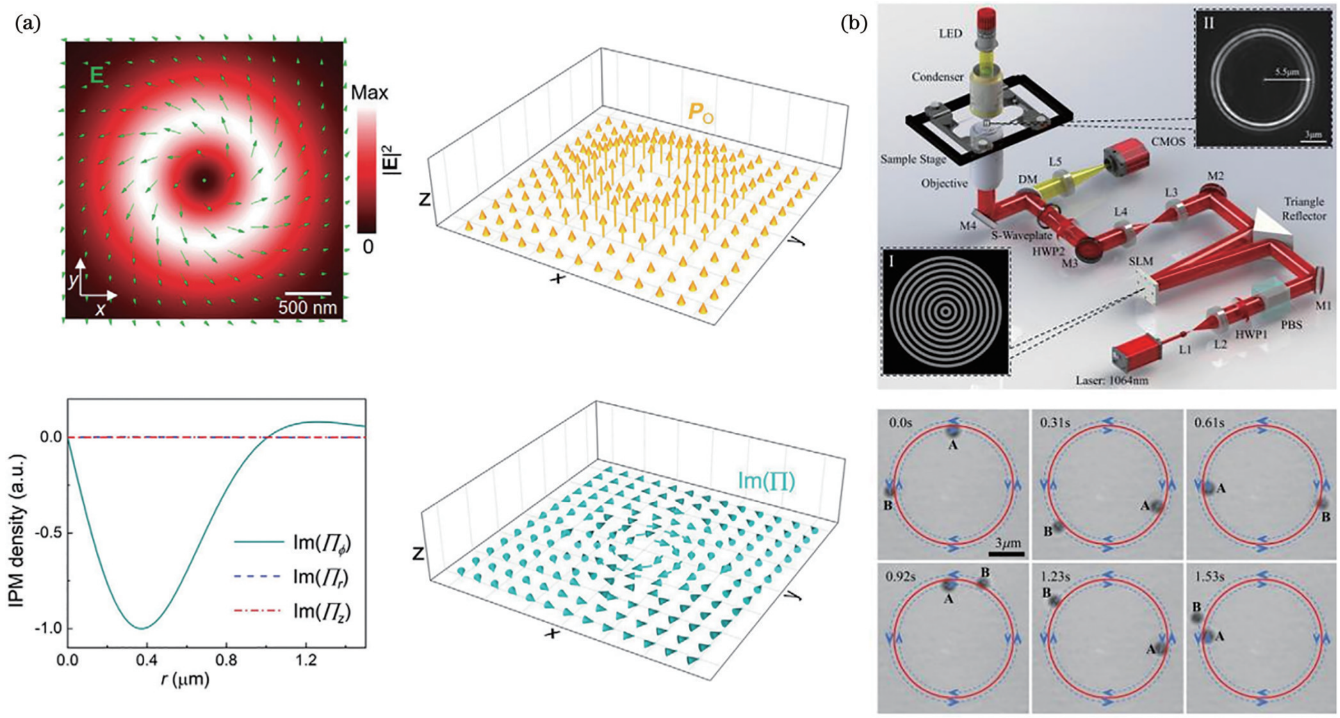

图 9 来自方位角 IPM 的 OLF。（a）IPM 涡旋波束中的场结构[32]；（b）由 IPM 诱导的 OLF 的实验观察[86]

Fig. 9 OLF from azimuthal IPM. (a) Field structure in IPM vortex beam[32]; (b) experimental observation of OLF induced by IPM[86]

IPM 不仅丰富了光学操控的自由度，它也对洛伦兹力的第一原理即 Maxwell 应力张量（MST）定理[146]有影响。最近，Nieto-Vesperinas 和 Xu[147]推导出了 IPM 的守恒方程，类似于著名的复数 Poynting 理论，在守恒方程的基础上将 MST 扩展到它的虚值。这种复杂的 MST 将是一个值得电动力学与光子学领域中的工作者们持续研究的课题[148]。

3.4 自旋-轨道相互作用产生的横向光力

近年来，由于 SOI 具有一些有趣的物理特性和广泛的应用，引起研究者们极大的关注。SOI 是一种描述光的自旋动量和轨道动量相耦合的现象。在耦合中，SAM 可以转换为 OAM，反之亦然。SOI 存在于紧密聚焦的高斯光场或是通过纳米颗粒存在于散射光场中。SOI 与 OLF 也有一定的联系。

SOI 在聚焦光中产生螺旋相关的涡旋[149-150]，如图 10（a）所示，这种涡旋能够产生光力，并诱导横向轨道绕光束轴旋转，这种光力与轨道动量 $\boldsymbol{p}_{\mathrm{o}}$ 相关，因此也与螺旋度所依赖的内在 OAM 相关。从根本上说，这个力与横向能量流有关，因此不能被归类为 OLF。而界面附近的 SOI 则可以在位于界面上方或界面处的粒子上产生光的不对称散射，进而产生一个 OLF[78]，如图 10（b）所示。对于位于界面上的粒子以及入射光

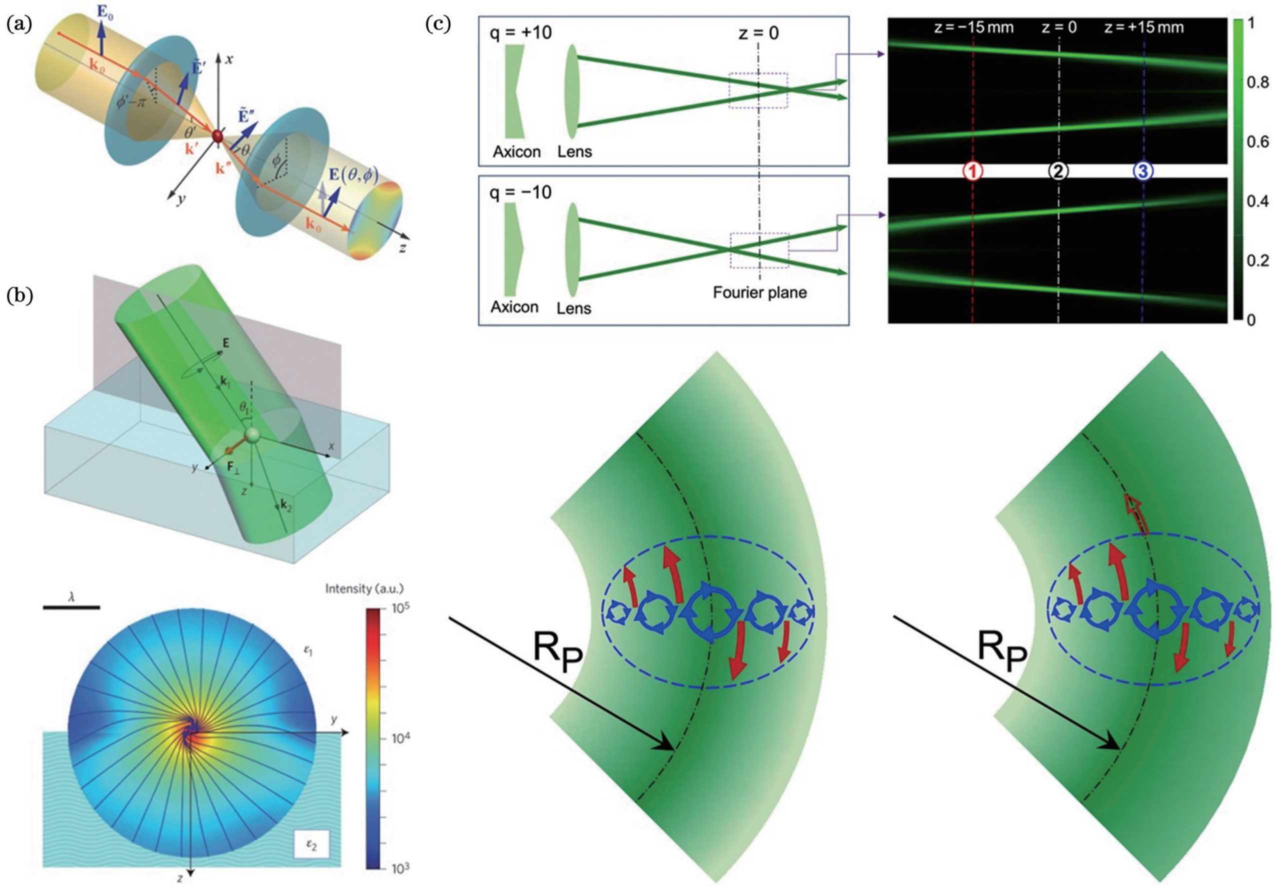

图 10 远场 SOI 产生的 OLF。(a)在强聚焦的光束中产生 SOI[150];(b)放置在空气和水界面的介电粒子上由于 SOI 产生 OLF[78];(c)环状光场中 SAM 向 OAM 的转换产生 OLF[154]

Fig. 10 OLF generated by SOI in far field. (a) Generation of SOI in highly focused beam[150]; (b) OLF on dielectric particles placed at air-water interface resulted from SOI[78]; (c) SAM-to-OAM conversion generates OLF in annular beam[154]

波场 $\boldsymbol{E}$,在表面附近的电偶极粒子上的力[18,28,151-153]可表示为

$$\langle \boldsymbol{F} \rangle = \frac{1}{2}\mathrm{Re}\left[\boldsymbol{d}^{*}\cdot\nabla\boldsymbol{E}\right] + \frac{1}{2}\mathrm{Re}\left[\boldsymbol{d}^{*}\cdot\nabla\boldsymbol{E}_{\mathrm{D}}\right], \quad (30)$$

式中:$\boldsymbol{E}_{\mathrm{D}}$为散射光场;$\boldsymbol{d}=\hat{\alpha}_{\mathrm{eff}}\boldsymbol{E}$为表面附近诱导的偶极矩,其中$\hat{\alpha}_{\mathrm{eff}}$为有效极化率。可以用对角格林张量$G_{\mathrm{jj}}$来解释粒子与表面的相互作用,也可以用对角格林张量$G_{\mathrm{jj}}$来表示$\hat{\alpha}_{\mathrm{eff}}$,具体表达式为

$$\hat{\alpha}_{\mathrm{eff}} = \frac{\alpha_{\mathrm{e}}}{1-\omega^{2}\mu_{1}\mu_{0}G_{\mathrm{jj}}(\boldsymbol{r}_{0},\boldsymbol{r}_{0}')\alpha_{\mathrm{e}}}, \quad (31)$$

式中:μ_1为颗粒的相对磁导率;$G_{\mathrm{jj}}(\boldsymbol{r}_0,\boldsymbol{r}_0')$为对角格林张量,其中$\boldsymbol{r}_0$为场点位置,$\boldsymbol{r}_0'$为源点位置。

当用倾斜入射的 CPL 照射颗粒时,垂直于入射平面的横向光强和 Poynting 动量的分布由于 SOI 的存在而变得不对称。界面的存在打破了光场分布的对称性,从而在颗粒上产生了 OLF。最近,Huang 等[154]研究了径向强度梯度光束中自旋到轨道动量的转换。如图 10(c)所示,光束产生一个线性变化的径向相位来控制 SAM,并在这个没有固有 OAM 的光阱中诱导了粒子的轨道运动。由于存在电、磁诱导的偶极子的干扰,这里的横向自旋动量$\boldsymbol{p}_{\mathrm{s}}$可以产生 OLF,但除此之外,强聚焦的光场还可以诱导强 SOI 去产生轨道动量$\boldsymbol{p}_{\mathrm{o}}$以及 OLF。

Rodríguez-Fortuño 等[79]通过将任意小的散射体(包括非手性、中心对称粒子或原子)放置在一个支持近场导模且单向激发的表面上,发现了与极化相关的横向反冲力,如图 11(a)所示。除了广泛研究的电自旋轨道耦合外,Fu 等[33]最近提出了一种一维介电光子晶体超表面激发光的磁自旋轨道耦合,可产生单向 Bloch 表面波,从而在粒子上产生 OLF,如图 11(b)所示。该 OLF 可由光螺旋度、粒子与表面之间的间隙和粒子大小来控制。

除了使用聚焦光束和界面,纳米结构也会产生强 SOI,从而产生 OLF[80],如图 11(c)所示。当被 CPL 照射时,波导和附近粒子之间会发生 SOI,从而产生 OLF。OLF 的方向和大小与光螺旋度和粒子位置直接相关。波导也可以弯曲形成一个环,使粒子在环形轨道上运动。这种方法可以避免使用锥形光纤[45-46]或光栅耦合器[155-156],并精确耦合光使其满足波导的需要,为片上光镊提供一种新方法。

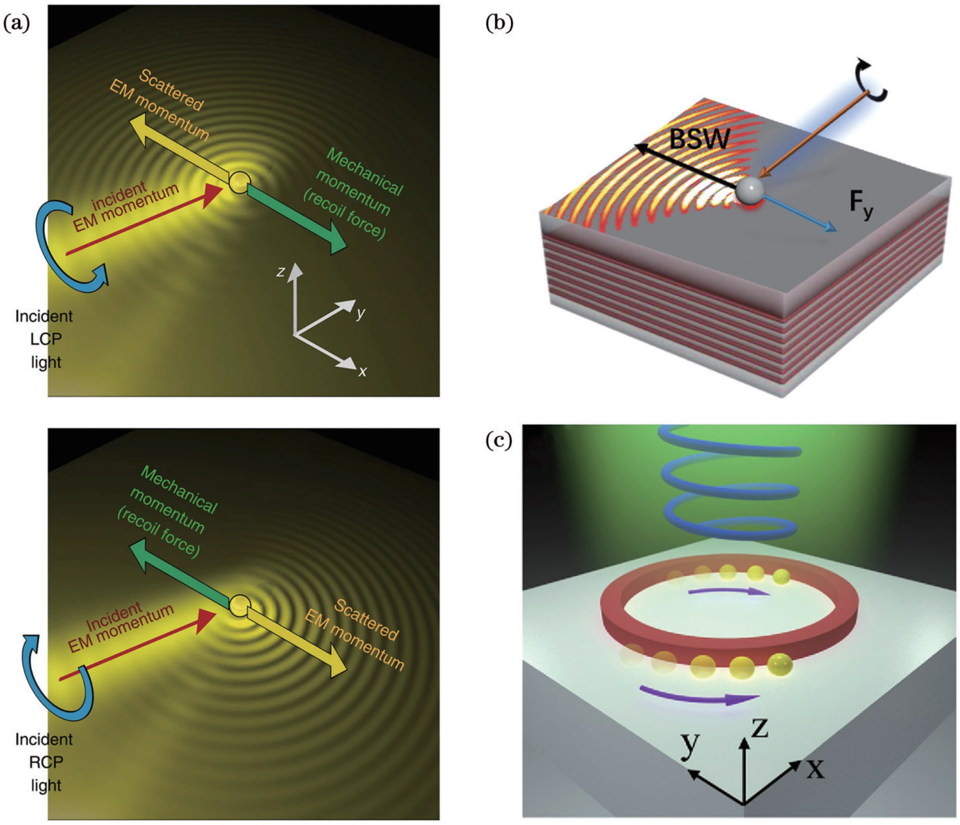

图 11 近场 SOI 产生的 OLF。(a)利用 CPL 打破对称性来激发横向 SPP 波和 OLF 示意图[79];(b)一维光子晶体结构产生的 OLF 通过粒子的磁共振模式进行调谐[33];(c)在 CPL 的照射下,当粒子在波导的上方或下方时粒子双向移动或沿着弯曲的波导旋转[80]

Fig. 11 OLF generated by SOI in near field. (a) Schematic diagram of using CPL to break symmetry and excite transverse SPP wave and OLF[79]; (b) OLF generated by one-dimensional photonic crystal structure being tuned via particle's magnetic resonance mode[33]; (c) under illumination of CPL, particles move bidirectionally or rotate along curved waveguide when placed above or below waveguide[80]

3.5 其他效应产生的横向力

本节介绍产生 OLF 的其他方法,尤其简要概述热效应、气泡或光拓扑对 OLF 的影响。将光力和其他辅助力结合起来,可以为光学操作、生物传感或微机械等多种应用提供了功能更强大的工具。

3.5.1 源于微泡的横向力

气泡是一种因加热而导致温度超过液体沸点所形成的气体空穴。当气泡的大小可以控制时,可以利用表面张力、气体压力、马兰戈尼对流和衬底粘附[157]来操控颗粒,将纳米颗粒排列为任意图案,如图 12(a)所示。这种技术被称为“气泡笔光刻”,它在高效和精确颗粒操控[157-162]、传感[159,163-165]和微驱动[166-167]等领域都有很好的应用。例如,Wang 等[166]利用金属纳米颗粒在微型涡轮叶片上进行沉积,使微型涡轮以 16 rad/s 的速度转动,如图 12(b)所示。此外,还在水蚤的胸部附属物上印制了磁铁,从而捕捉水蚤并使水蚤发生旋转。此外,Karim 等[168]利用微泡将金纳米颗粒沉积在固体表面,并将分析物引导到纳米颗粒区域进行传感,如图 12(c)所示。与被动传感方法相比,这种主动传感方法可以显著提高物质的检测灵敏度,为精密生化传感开辟了新途径。

3.5.2 热效应引起的横向力

由于没有一种材料能够完全不吸收光,所以很难避免热效应,但可以通过介电质材料来减弱热效应。热效应通常对光镊有负面影响,尽管中等激光强度或全介电材料的损耗可以忽略不计,但当使用金属激发等离子体共振的等离子体光镊时,加热现象可能会非常明显并对颗粒有害。热梯度可以驱动粒子运动,这种现象被称为热电泳效应,这是一个典型的非平衡输运问题[169]。激光束加热金属板会产生热梯度,导致粒子远离激光[170-171],如图 13(a)所示。热泳力的大小[75,172-174]可近似表示为

$$F_T = -\frac{9\pi a\eta^2 \Delta T}{\rho T\left(2 + C_m/C_p\right)}, \tag{32}$$

式中:C_p 为颗粒的导热系数;ρ、η、C_m、T 和 ΔT 分别为介质的密度、黏度、导热系数、温度和温度梯度;a 为颗粒半径。由式(32)可知,热泳力与温度梯度成正比,使粒子从高温区域移向低温区域。热泳力来源于颗粒边

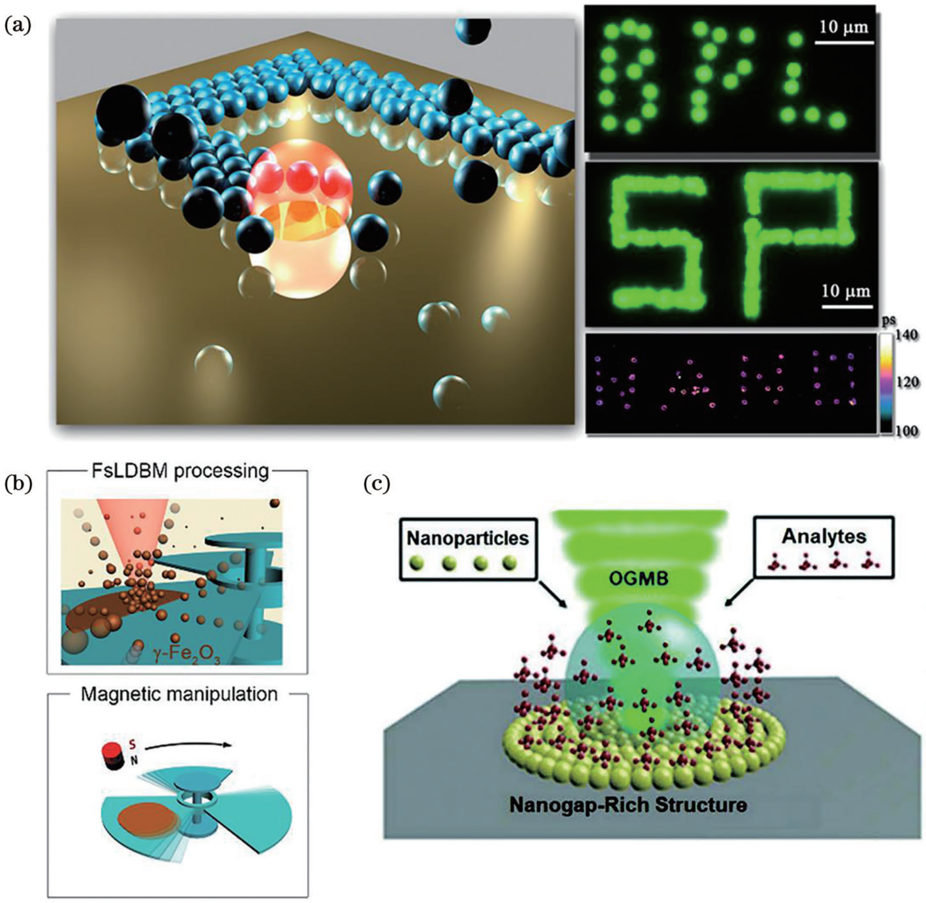

图 12 微泡中的横向力。(a)微泡捕获纳米颗粒机理[157];(b)利用微泡压缩打印技术实现可驱动微机械[166];(c)利用光热产生的微泡实现主动传感[168]

Fig. 12 Lateral force from microbubbles. (a) Mechanism of microbubble capturing nanoparticle[157]; (b) using microbubble compression printing technique can drive micromechanical motion[166]; (c) using microbubble generated by photothermal effect can achieve active sensing[168]

界处的滑移流,而当有底物存在时,也会产生类似的热渗流[170,175-177],如图 13(b)所示。

除了热电泳效应外,还有一种由流体内部各部分温度不同而引起的流动被称为对流,它是流体分子的一种运动方式,其流动路径与热渗流相类似[178],如图 13(c)所示。对流可以分为自然对流和马兰戈尼对流[158,179-183],理论分析表明,对流通常比热透和热渗流要小得多[170]。

流体阻力的表达式为 $\boldsymbol{F}_{\mathrm{drag}}=6f_{\mathrm{D}}\pi\eta a\boldsymbol{v}$,其中 $\boldsymbol{v}$ 是颗粒的速度,f_{D} 是阻力系数,与上下介质的黏度比有关[184]。当颗粒完全浸没在液体中时,$f_{\mathrm{D}}=1$;当颗粒处于两种介质的交界处时,$f_{\mathrm{D}}<1$。适当利用流体阻力,可快速且有效地操控颗粒[39-40,185-187]。

利用这三种热诱导流与其他力(如光力等)的结合,可以为颗粒操控增加一个自由度,从而显著扩大和提高捕集的范围、刚度和速度。Ndukaife 等[188]和 Chen 等[189]将交流电场加入到等离子光镊中,可根据电热效应产生涡流,快速地将纳米粒子输送到等离子体热点处,为芯片级的低功耗和远距离的光流体操控提供了一种有利的工具,如图 13(d)所示。由浮力和电场力共同驱动的诱导流的速度可以达到 10 μm/s,远远超过了之前所报道的对流速度[83]。

在最新的一项研究中,Lin 等[160,190-192]提出利用十六烷基三甲基氯化铵修饰纳米颗粒的表面,使其带正电,该方法可以在单个金属纳米颗粒的水平上进行操纵。这一创新技术被称为光热电纳米镊子,它可以高精度地操控不同尺寸、材料和形状的金属纳米颗粒,如图 13(e)所示。当激光束照射时,由于加热产生的流动(包括热泳、热渗透和对流)会排斥带负电荷的离子并产生电流,从而把带正电荷的金属纳米颗粒吸引到温度较高位置处。在这种情况下,微尺度的流体运动是由单个等离子体纳米结构引起的电热质流所导致的。另一方面,当用激光束照射 Janus 粒子时,会在聚苯乙烯-金一侧之间产生温度差[190]。当 Janus 粒子分散在十六烷基-三甲基氯化铵溶液中时,它们会自发地沿着温度梯度方向运动。Janus 粒子也可以通过旋转不对称加热引起的平面来控制其光学扭矩。这种特殊的光热微马达具有低激光功率需求、非侵入性、对尺寸

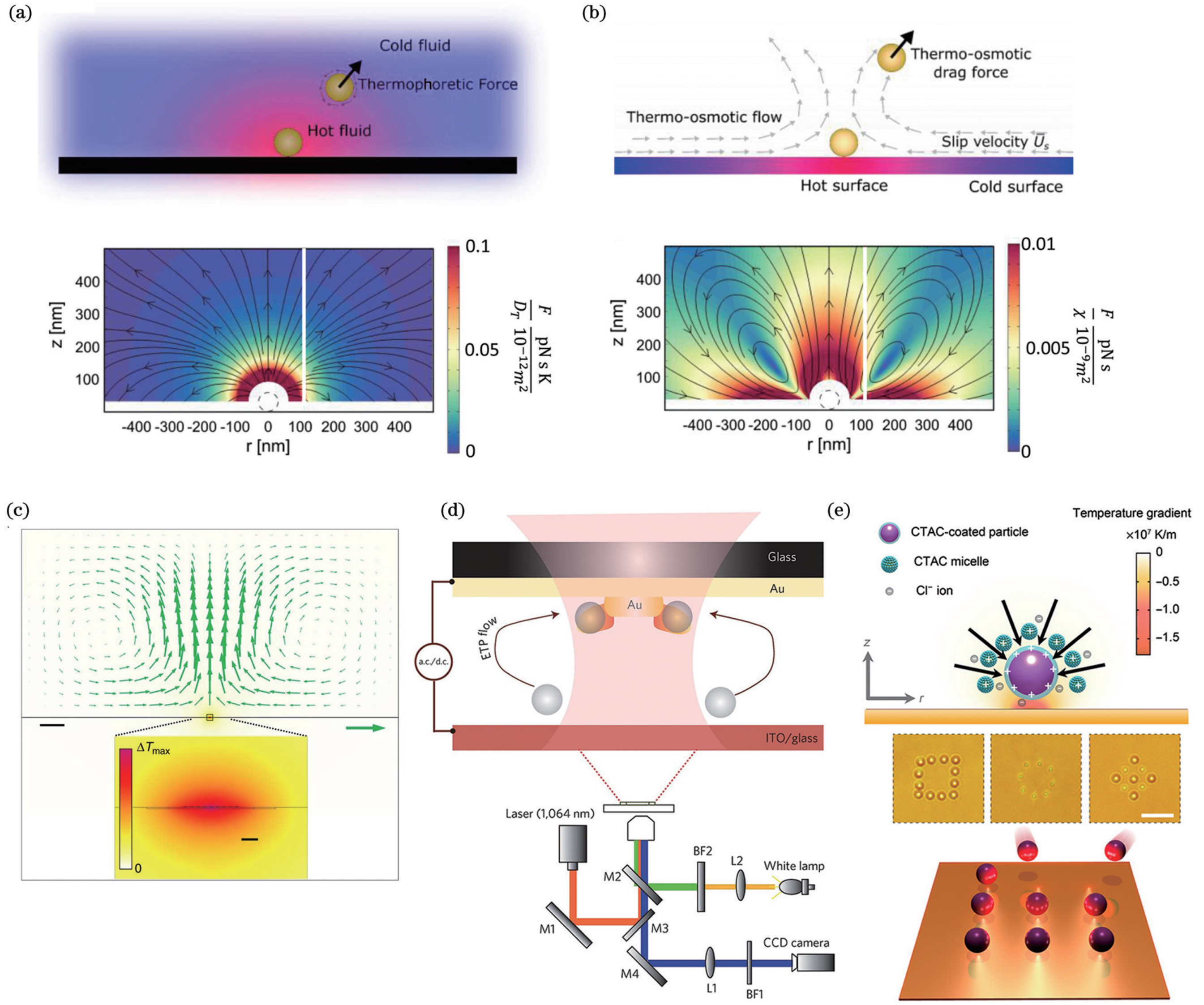

图 13 热诱导 OLF。(a)温度梯度引起的热泳力将粒子从高温区驱动到低温区[170]；(b)由表面温度梯度引起的滑移速度产生的热渗透力[170]；(c)氧化铟锡衬底上的金纳米天线产生强流体对流[178]；(d)与交流电场相结合的纳米天线加热实现颗粒操控示意图[188]；(e)粒子热电力操纵示意图[192]

Fig. 13 Heating-induced OLF. (a) Thermophoretic force caused by temperature gradient, which drives particle from high temperature region to low temperature region[170]; (b) thermo-osmosis force caused by slip velocity generated by surface temperature gradient[170]; (c) strong fluid convection generated by heating gold nanorod on indium tin oxide substrate[178]; (d) schematic diagram of nanoantenna heating combined with alternating electric field for particle manipulation[188]; (e) schematic diagram of manipulation of particles using thermoelectric force[192]

和形状不敏感以及波长可选等优点，有望成为光学操控纳米物体的有力工具。

3.5.3 其他横向力

简要回顾对 OLF 有重要影响但研究较少的一些因素。

拓扑光力是一种由光的拓扑特性引起的光力，它可以在与光传播方向垂直的平面上操纵粒子[193]。最近，Qin 等[194]利用双层光子晶体(PhCS)板实现了一种拓扑光力，它可以在与光传播方向垂直的平面上捕获、排斥和旋转粒子，如图 14 所示。当上下层结构无扭转，即上下层光子晶体旋转角 α_{top} 和 α_{bot} 相等时，光子能带的南北极线性偏振极点处存在两个 BIC 点，颗粒到达这两点时会被捕获到或被排斥出光束中心。当上下层结构存在扭转角，即上下层光子晶体旋转角 α_{top} 和 α_{bot} 不相等时，颗粒若位于南北极椭圆偏振极点处的 BIC 点，还会受到绕着光束中心旋转的扭矩作用从而发生绕轴旋转。这一理论研究揭示了一种与光拓扑相关的新型光力，这为开发特殊的拓扑光力提供了可能性，从而能够在物理和生物科学中为粒子操纵的许多应用增添新的功能。

在磁光表面附近放置偶极子是激发 OLF 的常见方法。当偶极子是线偏振而表面互易时，OLF 不存

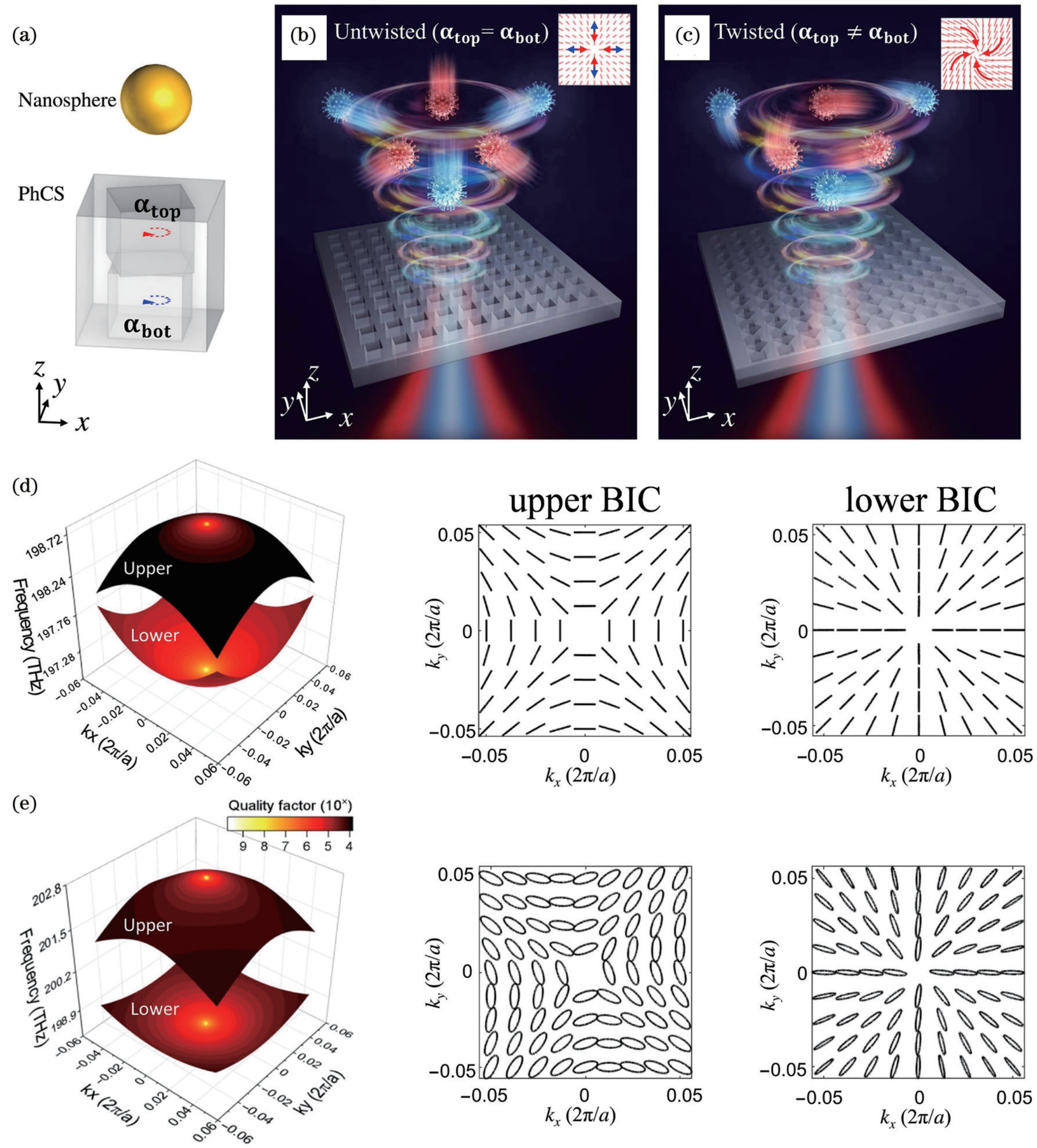

图 14　拓扑 OLF[194]。(a)产生拓扑光力的双层 PhCS 示意图；(b)当 $\alpha_{top}=\alpha_{bot}$ 时，PhCS 中的 BIC 模式操控颗粒示意图；(c)当 $\alpha_{top}\neq\alpha_{bot}$ 时，PhCS 中的 BIC 模式操控颗粒示意图；(d)当 $\alpha_{top}=\alpha_{bot}$ 时，能带结构及颗粒运动图；(e)当 $\alpha_{top}\neq\alpha_{bot}$ 时，能带结构及颗粒运动图

Fig. 14　Topological OLF[194]. (a) Schematic of double-layer PhCS that generates topological optical; (b) schematic of particle manipulation at BIC modes in PhCS when $\alpha_{top}=\alpha_{bot}$; (c) schematic of particle manipulation at BIC modes in PhCS when $\alpha_{top}\neq\alpha_{bot}$; (d) band structure and particle motion diagram when $\alpha_{top}=\alpha_{bot}$; (e) band structure and particle motion diagram when $\alpha_{top}\neq\alpha_{bot}$

在。但是，当表面非互易时[195-197]，由于光子拓扑绝缘体[198-200]和磁化等离子体[201]中的界面上存在单向传播的模式，此时可产生 OLF。即使外磁场方向与磁光表面相互垂直，线偏振的粒子在磁光表面附近也会产生 OLF[35]。偶极子的横向表面等离子体激元激发可以通过磁光材料的极化转换而改变，从而产生 OLF。

根据费米黄金规则，任一偶极子在表面附近的 OLF 都可以用角频谱来直观描述[202]。从傅里叶频谱可以看出，表面上方的惠更斯偶极子主要受到 SPP 中 OLF 的影响。这种方法突出了反向散射场在计算偶极子上光力时的重要性。Li 等[203]报道了一种 Fano 干涉效应，它可以在等离子纳米粒子上产生强烈的不对称侧向散射，从而产生显著增强的 OLF。这种力可以推广到各种等离子体纳米结构，并将其作为一种灵敏的光学分选方法。

超光镊是一种利用超表面来操纵光场的技术，

它使用了具有超材料结构的器件，展现了对粒子的非凡控制能力[28]。最近，Paul等[152]利用双曲和各向异性超表面，可以使超约束表面等离子体激元与粒子的面外偏振自旋之间实现强烈的相互作用，从而产生增强的OLF。这种OLF对制造误差和入射波长具有很好的鲁棒性，并且对损耗具有一定的容忍性，适用于纳米操作或传感的多种场合。利用相变纳米天线，可以在10 nm以下的纳米颗粒上获得巨大的可调谐OLF[204]，进一步突破了产生OLF的颗粒尺寸极限。

在光流体对粒子的操作中，一个很重要但容易被忽略的力是Magnus力或升力，它作用于同时移动和旋转的粒子[205-207]。这个Magnus力[205,208]具体表达式为

$$\boldsymbol{F}_{\text{Magnus}} = \pi a^3 \rho \boldsymbol{\varphi} \times \boldsymbol{v}\left[1 + O(Re)\right], \tag{33}$$

式中：$\boldsymbol{\varphi}$是颗粒的角速度，雷诺数$Re = \rho v a/\eta$，ρ和v分别是流体的密度和速度。在这种情况下，Magnus力可以视为横向力，它不是独立存在的。另一种常见的流体力是惯性升力，它已经广泛应用于细胞分选[209-214]，其表达式为

$$\boldsymbol{F}_{\text{L}} = C_{\text{L}} \rho \boldsymbol{v}_0^2 A/2, \tag{34}$$

式中：C_{L}为升力系数；$\boldsymbol{v}_0$是颗粒与流体之间的相对速度；A是正对流体流动方向的表面积。普遍存在的Magnus力和惯性升力也可能应用于细胞操控中。

3.6 横向光力的应用前景

近年来随着微纳光学的发展，OLF也得到了广泛研究。OLF的相关研究有望为光学操控带来诸多新机遇。

结构光为光学操控提供了巨大可能性。典型的例子包括贝塞尔光束中的光牵引力[11,15,39]、艾利光束实现的三维操控[215-217]或涡旋光束引起的颗粒旋转[218-220]。结构粒子[107]，例如Janus粒子[190,221-222]、核壳粒子[140,223-224]、手性粒子[47,225]、上转换粒子[226]、三角棱镜[226-228]或缺陷粒子[229]等均被广泛用于增强OLF和赋予光镊各种特殊功能。超表面在电磁波操控方面展示出的前所未有的优势[230-239]，也为操纵粒子提供了更多新的可能。特别是随着纳米制造技术的快速发展，出现了一种由OLF驱动的“超构机器人”（Meta-robot）[28,142,240]。通过调控光的偏振、波长等参数，可以在自由运动的超表面上施加光力（如OLF），使得超表面（超构机器人）在二维或三维运动。最近，南京大学Li等[241]设计了一种基于相位梯度超表面产生OLF的多功能“Meta-vehicle”。该超构机器人虽然还没有在实际中使用，但有望将其应用于如生物颗粒运输、局部探测、细胞拉伸和生物治疗等生物医学领域[242]。OLF还有其他多种生物化学应用[243-244]，例如分选外泌体等生物颗粒、用双光束拉伸和折叠DNA或蛋白分子、用超构机器人传递和结合生物颗粒、手性探测以及螺旋二色性传感[245]等。

手性物体在自然界中广泛存在，例如DNA、氨基酸、蛋白质等[106]。实现手性对映体分离与传感一直以来都是人们所关注的重点[105]。例如，在2012年，Pu[246]利用1,1′-Bi-2,2′-Naphthol的独特结构构建了手性对映体选择性荧光传感器。在2020年，Solomon等[105]提出了通过设计金属和电介质纳米结构来提高光学手性密度的新策略。基于以上研究并结合OLF性质，有望在手性分子高灵敏度生化传感、对映体全光分离等方面取得新进展。手性光力为人们打开了许多新视角，并重新引发了人们关于手性在基本物理现象中能否扮演重要角色的讨论[247]。而手性光力与分子手性之间的一些潜在的特殊关联也为这一非常活跃的研究领域带来了许多想法。

尽管目前利用OLF进行的相关研究较少，但是人们对利用OLF进行光学操控、探索光学操控更多可能性的研究从未停止。未来OLF有望在分子物理学、光机械学、热力学、量子物理学、光学操纵和材料等学科中得到更广泛的应用。

4 总结与展望

动量和力是物理学中的两个基本概念，其纵向分量得到了广泛深入的研究，包括轨道动量以及CPL中的SAM等。电磁线性动量领域存在着著名的Abraham-Minkowski争议，其细节可以参阅文献[28, 78, 248-252]。光辐射压力的方向平行于光传播方向，光牵引力方向与光传播方向相反，这两种力都是纵向光力，在文献[15, 220, 253-257]中有详细的阐述。

横向动量在光操作、传感和光-物质相互作用等方面都扮演着重要角色，这与它可以诱导OLF密切相关。其中一种特殊的光力是自旋动量或BSM力，它平行于横向BSM，方向可根据颗粒材质的不同而发生改变。然而，相对于传统的OGF或散射力，这种力是非常微弱的，很难被检测到，因此通常被忽视。可以通过一些典型方法包括使用倏逝波、驻波和单一线状光束等来研究这种力。

横向SAM很难在非手性或非磁电粒子上产生OLF，但它可以通过光和手性的耦合在手性体上产生OLF。实际上，横向SAM诱导的作用在手性纳米颗粒上的OLF甚至可以超过Poynting动量或光辐射压力诱导的OLF。当粒子放置在表面附近时，由于界面可以产生SOI并诱导表面波，如全内反射的倏逝波或金属上的表面SPP等，从而产生OLF。此外，利用IPM也有可能在偶极子上实现OLF，这丰富了光学操控的自由度，也提供了有关光力机制的新理解。此外，利用各种其他效应（例如热效应、气泡、光拓扑等）也可以得到OLF。实际上，随着该研究领域的快速发展，近期还出现了许多产生OLF的新机制，例如，在2023年，Nan等[258]发现即使在线偏振平面波的照射下，非

手性细长纳米颗粒中的多级子相互作用也可以产生OLF，这种基于多极子作用的OLF的符号和大小可以通过光场的偏振方向、入射光的入射角和波长，以及粒子的长宽比和材料来调整。这些发现为粒子光学分选和光驱动微/纳米马达等光机械应用提供了有效的策略。这些相关机制有望为今后的光学操控提供更加广泛且实用的工具[259-262]。

随着横向光动量（有时也称为异常光动量）光学模型的创新和完善，对OLF机制的理解正在不断深入。这些横向光动量也包括最近提出的横向SAM[30,120,263-267]，skyrmions和merons[268-272]等。因此光力也成为了测试和应用诸多包括横向动量在内的特殊光学现象的关键平台和有效工具[185,273-280]。

传统的OGF和光辐射压力在过去的几十年中已经被广泛研究，与此同时，它们在一些应用中的技术限制也同时被人们所认识到。近年来发现的一些奇特光力，如光牵引力和OLF，在高精度操作中发挥着越来越重要的作用。在光牵引力方面，读者可以参考先前所发表的关于光牵引力的长篇综述[15]。

总而言之，随着现代微纳光学和光子学的发展，动量和力这两个相互关联的物理量已经得到了深入的探索，并且将在生物医学、量子物理、自旋光子、化学合成、光机械等领域中得到更广泛的应用。

参 考 文 献

[1] Ashkin A, Dziedzic J M, Bjorkholm J E, et al. Observation of a single-beam gradient force optical trap for dielectric particles[J]. Optics Letters, 1986, 11(5): 288-290.

[2] Phillips W D. Nobel Lecture: laser cooling and trapping of neutral atoms[J]. Reviews of Modern Physics, 1998, 70(3): 721-741.

[3] Dalibard J, Cohen-Tannoudji C. Laser cooling below the Doppler limit by polarization gradients: simple theoretical models [J]. Journal of the Optical Society of America B, 1989, 6(11): 2023-2045.

[4] Chu S, Hollberg L, Bjorkholm J E, et al. Three-dimensional viscous confinement and cooling of atoms by resonance radiation pressure[J]. Physical Review Letters, 1985, 55(1): 48-51.

[5] Kasevich M, Chu S. Laser cooling below a photon recoil with three-level atoms[J]. Physical Review Letters, 1992, 69(12): 1741-1744.

[6] Lett P D, Watts R N, Westbrook C I, et al. Observation of atoms laser cooled below the Doppler limit[J]. Physical Review Letters, 1988, 61(2): 169-172.

[7] Mitra D, Vilas N B, Hallas C, et al. Direct laser cooling of a symmetric top molecule[J]. Science, 2020, 369(6509): 1366-1369.

[8] Shi Y Z, Liu A Q, Qiu C W, et al. Research progress on optofluidic optical tweezers[J]. Optics and Precision Engineering, 2022, 30(21): 2765-2782.

[9] Zhu Z, Zhang Y Q, Zhang S S, et al. Nonlinear optical trapping effect with reverse saturable absorption[J]. Advanced Photonics, 2023, 5(4): 046006.

[10] Pu J J, Zeng K, Wu Y L, et al. Miniature optical force levitation system[J]. Chinese Optics Letters, 2022, 20(1): 013801.

[11] Chen J, Ng J, Lin Z F, et al. Optical pulling force[J]. Nature Photonics, 2011, 5: 531-534.

[12] Li H, Cao Y Y, Shi B J, et al. Momentum-topology-induced optical pulling force[J]. Physical Review Letters, 2020, 124(14): 143901.

[13] Brzobohatý O, Karásek V, Šiler M, et al. Experimental demonstration of optical transport, sorting and self-arrangement using a 'tractor beam'[J]. Nature Photonics, 2013, 7: 123-127.

[14] Novitsky A, Qiu C W, Wang H F. Single gradientless light beam drags particles as tractor beams[J]. Physical Review Letters, 2011, 107(20): 203601.

[15] Li H, Cao Y Y, Zhou L M, et al. Optical pulling forces and their applications[J]. Advances in Optics and Photonics, 2020, 12(2): 288-366.

[16] Li X, Chen J, Lin Z F, et al. Optical pulling at macroscopic distances[J]. Science Advances, 2019, 5(3): eaau7814.

[17] Wang N, Lu W L, Ng J, et al. Optimized optical "tractor beam" for core-shell nanoparticles[J]. Optics Letters, 2014, 39(8): 2399-2402.

[18] Petrov M I, Sukhov S V, Bogdanov A A, et al. Surface plasmon polariton assisted optical pulling force[J]. Laser & Photonics Reviews, 2016, 10(1): 116-122.

[19] Mahdy M R C, Zhang T H, Das S C, et al. On chip optical tractor beam by surface plasmon polariton[J]. Optics Communications, 2020, 463: 125395.

[20] Zhang Y Q, Min C J, Dou X J, et al. Plasmonic tweezers: for nanoscale optical trapping and beyond[J]. Light, Science & Applications, 2021, 10(1): 59.

[21] Roxworthy B J, Ko K D, Kumar A, et al. Application of plasmonic bowtie nanoantenna arrays for optical trapping, stacking, and sorting[J]. Nano Letters, 2012, 12(2): 796-801.

[22] Jin R C, Xu Y H, Dong Z G, et al. Optical pulling forces enabled by hyperbolic metamaterials[J]. Nano Letters, 2021, 21 (24): 10431-10437.

[23] Shalin A S, Sukhov S V, Bogdanov A A, et al. Optical pulling forces in hyperbolic metamaterials[J]. Physical Review A, 2015, 91(6): 063830.

[24] Lepeshov S, Krasnok A. Virtual optical pulling force[J]. Optica, 2020, 7(8): 1024-1030.

[25] Lee E, Luo T. Long-distance optical pulling of nanoparticle in a low index cavity using a single plane wave[J]. Science Advances, 2020, 6(21): eaaz3646.

[26] Poynting J H. The wave motion of a revolving shaft, and a suggestion as to the angular momentum in a beam of circularly polarised light[J]. Proceedings of the Royal Society of London Series A: Containing Papers of a Mathematical and Physical Character, 1909, 82(557): 560-567.

[27] Allen L, Beijersbergen M W, Spreeuw R J, et al. Orbital angular momentum of light and the transformation of Laguerre-Gaussian laser modes[J]. Physical Review A, 1992, 45(11): 8185-8189.

[28] Shi Y Z, Song Q H, Toftul I, et al. Optical manipulation with metamaterial structures[J]. Applied Physics Reviews, 2022, 9 (3): 031303.

[29] Shen Y J, Wang X J, Xie Z W, et al. Optical vortices 30 years on: OAM manipulation from topological charge to multiple singularities[J]. Light, Science & Applications, 2019, 8: 90.

[30] Bliokh K Y, Bekshaev A Y, Nori F. Extraordinary momentum and spin in evanescent waves[J]. Nature Communications, 2014, 5: 3300.

[31] Bekshaev A Y, Bliokh K Y, Nori F. Transverse spin and momentum in two-wave interference[J]. Physical Review X, 2015, 5(1): 011039.

[32] Xu X H, Nieto-Vesperinas M. Azimuthal imaginary Poynting momentum density[J]. Physical Review Letters, 2019, 123(23): 233902.

[33] Fu Y N, Zhang Y Q, Min C J, et al. Lateral forces on particles induced by magnetic spin-orbit coupling[J]. Optics Express,

2020, 28(9): 13116-13124.
[34] Hayat A, Mueller J P, Capasso F. Lateral chirality-sorting optical forces[J]. Proceedings of the National Academy of Sciences of the United States of America, 2015, 112(43): 13190-13194.
[35] Girón-Sedas J A, Kingsley-Smith J J, Rodríguez-Fortuño F J. Lateral optical force on linearly polarized dipoles near a magneto-optical surface based on polarization conversion[J]. Physical Review B, 2019, 100(7): 075419.
[36] Yang B, Sun H, Huang C J, et al. Cooling and entangling ultracold atoms in optical lattices[J]. Science, 2020, 369(6503): 550-553.
[37] Kaufman A M, Lester B J, Regal C A. Cooling a single atom in an optical tweezer to its quantum ground state[J]. Physical Review X, 2012, 2(4): 041014.
[38] Kastberg A, Phillips W D, Rolston S L, et al. Adiabatic cooling of cesium to 700 nK in an optical lattice[J]. Physical Review Letters, 1995, 74(9): 1542-1545.
[39] Shi Y Z, Xiong S, Chin L K, et al. Nanometer-precision linear sorting with synchronized optofluidic dual barriers[J]. Science Advances, 2018, 4(1): eaao0773.
[40] Shi Y Z, Xiong S, Zhang Y, et al. Sculpting nanoparticle dynamics for single-bacteria-level screening and direct binding-efficiency measurement[J]. Nature Communications, 2018, 9(1): 815.
[41] Wang M M, Tu E, Raymond D E, et al. Microfluidic sorting of mammalian cells by optical force switching[J]. Nature Biotechnology, 2005, 23(1): 83-87.
[42] Tkachenko G, Brasselet E. Optofluidic sorting of material chirality by chiral light[J]. Nature Communications, 2014, 5: 3577.
[43] Shi Y Z, Li Z Y, Liu P Y, et al. On-chip optical detection of viruses: a review[J]. Advanced Photonics Research, 2021, 2(4): 2000150.
[44] Ashkin A, Dziedzic J M. Optical trapping and manipulation of viruses and bacteria[J]. Science, 1987, 235(4795): 1517-1520.
[45] Shi Y Z, Zhao H T, Chin L K, et al. Optical potential-well array for high-selectivity, massive trapping and sorting at nanoscale[J]. Nano Letters, 2020, 20(7): 5193-5200.
[46] Shi Y Z, Zhao H T, Nguyen K T, et al. Nanophotonic array-induced dynamic behavior for label-free shape-selective bacteria sieving[J]. ACS Nano, 2019, 13(10): 12070-12080.
[47] Shi Y Z, Wu Y F, Chin L K, et al. Multifunctional virus manipulation with large-scale arrays of all-dielectric resonant nanocavities[J]. Laser & Photonics Reviews, 2022, 16(5): 2100197.
[48] MacDonald M P, Spalding G C, Dholakia K. Microfluidic sorting in an optical lattice[J]. Nature, 2003, 426(6965): 421-424.
[49] Danesh M, Zadeh M J, Zhang T H, et al. Monolayer conveyor for stably trapping and transporting sub-1 nm particles[J]. Laser & Photonics Reviews, 2020, 14(8): 2000030.
[50] Zheng Y X, Ryan J, Hansen P, et al. Nano-optical conveyor belt, part II: demonstration of handoff between near-field optical traps[J]. Nano Letters, 2014, 14(6): 2971-2976.
[51] Hansen P, Zheng Y X, Ryan J, et al. Nano-optical conveyor belt, part I: theory[J]. Nano Letters, 2014, 14(6): 2965-2970.
[52] Nan F, Yan Z J. Sorting metal nanoparticles with dynamic and tunable optical driven forces[J]. Nano Letters, 2018, 18(7): 4500-4505.
[53] Jákl P, Čižmár T, Šerý M, et al. Static optical sorting in a laser interference field[J]. Applied Physics Letters, 2008, 92(16): 161110.
[54] Cong H J, Loo J, Chen J J, et al. Target trapping and *in situ* single-cell genetic marker detection with a focused optical beam[J]. Biosensors and Bioelectronics, 2019, 133: 236-242.
[55] Wang M D, Yin H, Landick R, et al. Stretching DNA with optical tweezers[J]. Biophysical Journal, 1997, 72(3): 1335-1346.
[56] Li J, Dao M, Lim C T, et al. Spectrin-level modeling of the cytoskeleton and optical tweezers stretching of the erythrocyte[J]. Biophysical Journal, 2005, 88(5): 3707-3719.
[57] Bennink M L, Leuba S H, Leno G H, et al. Unfolding individual nucleosomes by stretching single chromatin fibers with optical tweezers[J]. Nature Structural Biology, 2001, 8(7): 606-610.
[58] Zhang H, Liu K K. Optical tweezers for single cells[J]. Journal of the Royal Society: Interface, 2008, 5(24): 671-690.
[59] Bustamante C J, Chemla Y R, Liu S X, et al. Optical tweezers in single-molecule biophysics[J]. Nature Reviews: Methods Primers, 2021, 1: 25.
[60] Comstock M J, Whitley K D, Jia H F, et al. Protein structure. Direct observation of structure-function relationship in a nucleic acid-processing enzyme[J]. Science, 2015, 348(6232): 352-354.
[61] Sudhakar S, Abdosamadi M K, Jachowski T J, et al. Germanium nanospheres for ultraresolution picotensiometry of kinesin motors[J]. Science, 2021, 371(6530): eabd9944.
[62] Desai V P, Frank F, Lee A, et al. Co-temporal force and fluorescence measurements reveal a ribosomal gear shift mechanism of translation regulation by structured mRNAs[J]. Molecular Cell, 2019, 75(5): 1007-1019.
[63] Le T T, Yang Y, Tan C, et al. Mfd dynamically regulates transcription via a release and catch-up mechanism[J]. Cell, 2018, 172(1/2): 344-357.
[64] Roichman Y, Sun B, Roichman Y, et al. Optical forces arising from phase gradients[J]. Physical Review Letters, 2008, 100(1): 013602.
[65] Chin L K, Shi Y Z, Liu A Q. Optical forces in silicon nanophotonics and optomechanical systems: science and applications[J]. Advanced Devices & Instrumentation, 2020, 2020: 1964015.
[66] Chaumet P C, Nieto-Vesperinas M. Time-averaged total force on a dipolar sphere in an electromagnetic field[J]. Optics Letters, 2000, 25(15): 1065-1067.
[67] O'Neil A T, MacVicar I, Allen L, et al. Intrinsic and extrinsic nature of the orbital angular momentum of a light beam[J]. Physical Review Letters, 2002, 88(5): 053601.
[68] Arias-González J R, Nieto-Vesperinas M. Optical forces on small particles: attractive and repulsive nature and plasmon-resonance conditions[J]. Journal of the Optical Society of America A, 2003, 20(7): 1201-1209.
[69] Jesacher A, Maurer C, Schwaighofer A, et al. Full phase and amplitude control of holographic optical tweezers with high efficiency[J]. Optics Express, 2008, 16(7): 4479-4486.
[70] Jonás A, Zemánek P. Light at work: the use of optical forces for particle manipulation, sorting, and analysis[J]. Electrophoresis, 2008, 29(24): 4813-4851.
[71] Yan Z J, Sajjan M, Scherer N F. Fabrication of a material assembly of silver nanoparticles using the phase gradients of optical tweezers[J]. Physical Review Letters, 2015, 114(14): 143901.
[72] Shi Y Z, Zhu T T, Liu J Q, et al. Stable optical lateral forces from inhomogeneities of the spin angular momentum[J]. Science Advances, 2022, 8(48): eabn2291.
[73] Berry M V. Optical currents[J]. Journal of Optics A: Pure and Applied Optics, 2009, 11(9): 094001.
[74] Wang S B, Chan C T. Lateral optical force on chiral particles near a surface[J]. Nature Communications, 2014, 5: 3307.
[75] Shi Y Z, Zhu T T, Zhang T H, et al. Chirality-assisted lateral momentum transfer for bidirectional enantioselective separation[J]. Light, Science & Applications, 2020, 9: 62.
[76] Zhu T T, Shi Y Z, Ding W Q, et al. Extraordinary multipole

modes and ultra-enhanced optical lateral force by chirality[J]. Physical Review Letters, 2020, 125(4): 043901.
[77] Chen H J, Zheng H X, Lu W L, et al. Lateral optical force due to the breaking of electric-magnetic symmetry[J]. Physical Review Letters, 2020, 125(7): 073901.
[78] Sukhov S, Kajorndejnukul V, Naraghi R R, et al. Dynamic consequences of optical spin-orbit interaction[J]. Nature Photonics, 2015, 9: 809-812.
[79] Rodríguez-Fortuño F J, Engheta N, Martínez A, et al. Lateral forces on circularly polarizable particles near a surface[J]. Nature Communications, 2015, 6: 8799.
[80] Zhang Z B, Min C J, Fu Y N, et al. Controllable transport of nanoparticles along waveguides by spin-orbit coupling of light[J]. Optics Express, 2021, 29(4): 6282-6292.
[81] Zhang Q, Li J Q, Liu X G. Optical lateral forces and torques induced by chiral surface-plasmon-polaritons and their potential applications in recognition and separation of chiral enantiomers [J]. Physical Chemistry Chemical Physics: PCCP, 2019, 21(3): 1308-1314.
[82] Sukhov S, Dogariu A. Non-conservative optical forces[J]. Reports on Progress in Physics, 2017, 80(11): 112001.
[83] Quidant R, Girard C. Surface-plasmon-based optical manipulation[J]. Laser & Photonics Reviews, 2008, 2(1/2): 47-57.
[84] Albaladejo S, Marqués M I, Laroche M, et al. Scattering forces from the curl of the spin angular momentum of a light field[J]. Physical Review Letters, 2009, 102(11): 113602.
[85] Nieto-Vesperinas M, Xu X H. Reactive helicity and reactive power in nanoscale optics: evanescent waves. Kerker conditions. Optical theorems and reactive dichroism[J]. Physical Review Research, 2021, 3(4): 043080.
[86] Zhou Y, Xu X H, Zhang Y N, et al. Observation of high-order imaginary Poynting momentum optomechanics in structured light [J]. Proceedings of the National Academy of Sciences of the United States of America, 2022, 119(44): e2209721119.
[87] Nieto-Vesperinas M, Gomez-Medina R, Saenz J J. Angle-suppressed scattering and optical forces on submicrometer dielectric particles[J]. Journal of the Optical Society of America A, 2011, 28(1): 54-60.
[88] Nieto-Vesperinas M, Sáenz J J, Gómez-Medina R, et al. Optical forces on small magnetodielectric particles[J]. Optics Express, 2010, 18(11): 11428-11443.
[89] Chaumet P C, Rahmani A. Electromagnetic force and torque on magnetic and negative-index scatterers[J]. Optics Express, 2009, 17(4): 2224-2234.
[90] Bekshaev A Y. Subwavelength particles in an inhomogeneous light field: optical forces associated with the spin and orbital energy flows[J]. Journal of Optics, 2013, 15(4): 044004.
[91] Chen H J, Liang C H, Liu S Y, et al. Chirality sorting using two-wave-interference-induced lateral optical force[J]. Physical Review A, 2016, 93(5): 053833.
[92] Cipparrone G, Ricardez-Vargas I, Pagliusi P, et al. Polarization gradient: exploring an original route for optical trapping and manipulation[J]. Optics Express, 2010, 18(6): 6008-6013.
[93] Bliokh K Y, Nori F. Transverse and longitudinal angular momenta of light[J]. Physics Reports, 2015, 592: 1-38.
[94] García-Etxarri A, Gómez-Medina R, Froufe-Pérez L S, et al. Strong magnetic response of submicron silicon particles in the infrared[J]. Optics Express, 2011, 19(6): 4815-4826.
[95] Yevick A, Evans D J, Grier D G. Photokinetic analysis of the forces and torques exerted by optical tweezers carrying angular momentum[J]. Philosophical Transactions Series A: Mathematical, Physical, and Engineering Sciences, 2017, 375 (2087): 20150432.
[96] Svak V, Brzobohatý O, Šiler M, et al. Transverse spin forces and non-equilibrium particle dynamics in a circularly polarized vacuum optical trap[J]. Nature Communications, 2018, 9(1): 5453.
[97] Zhang T H, Mahdy M R C, Liu Y M, et al. All-optical chirality-sensitive sorting via reversible lateral forces in interference fields[J]. ACS Nano, 2017, 11(4): 4292-4300.
[98] Ginis V, Liu L L, She A L, et al. Using the Belinfante momentum to retrieve the polarization state of light inside waveguides[J]. Scientific Reports, 2019, 9(1): 14879.
[99] Antognozzi M, Bermingham C R, Harniman R L, et al. Direct measurements of the extraordinary optical momentum and transverse spin-dependent force using a nano-cantilever[J]. Nature Physics, 2016, 12: 731-735.
[100] Lu J S, Ginis V, Qiu C W, et al. Polarization-dependent forces and torques at resonance in a microfiber-microcavity system[J]. Physical Review Letters, 2023, 130(18): 183601.
[101] Liu L L, Di Donato A, Ginis V, et al. Three-dimensional measurement of the helicity-dependent forces on a Mie particle [J]. Physical Review Letters, 2018, 120(22): 223901.
[102] Zhou Y, Zhang Y N, Xu X H, et al. Optical forces on multipoles induced by the Belinfante spin momentum[J]. Laser & Photonics Reviews, 2023, 17(11): 2300245.
[103] Stilgoe A B, Nieminen T A, Rubinsztein-Dunlop H. Controlled transfer of transverse orbital angular momentum to optically trapped birefringent microparticles[J]. Nature Photonics, 2022, 16: 346-351.
[104] Yu X N, Li Y X, Xu B J, et al. Anomalous lateral optical force as a manifestation of the optical transverse spin[J]. Laser & Photonics Reviews, 2023, 17(10): 2300212.
[105] Solomon M L, Saleh A A E, Poulikakos L V, et al. Nanophotonic platforms for chiral sensing and separation[J]. Accounts of Chemical Research, 2020, 53(3): 588-598.
[106] Mun J, Kim M, Yang Y, et al. Electromagnetic chirality: from fundamentals to nontraditional chiroptical phenomena[J]. Light, Science & Applications, 2020, 9: 139.
[107] Zhou L M, Shi Y Z, Zhu X Y, et al. Recent progress on optical micro/nanomanipulations: structured forces, structured particles, and synergetic applications[J]. ACS Nano, 2022, 16 (9): 13264-13278.
[108] Yokota M, He S, Takenaka T. Scattering of a Hermite-Gaussian beam field by a chiral sphere[J]. Journal of the Optical Society of America A, 2001, 18(7): 1681-1689.
[109] Ding K, Ng J, Zhou L, et al. Realization of optical pulling forces using chirality[J]. Physical Review A, 2014, 89(6): 063825.
[110] Shi H S, Zheng H X, Chen H J, et al. Optical binding and lateral forces on chiral particles in linearly polarized plane waves [J]. Physical Review A, 2020, 101(4): 043808.
[111] Tkachenko G, Brasselet E. Helicity-dependent three-dimensional optical trapping of chiral microparticles[J]. Nature Communications, 2014, 5: 4491.
[112] Cipparrone G, Mazzulla A, Pane A, et al. Chiral self-assembled solid microspheres: a novel multifunctional microphotonic device [J]. Advanced Materials, 2011, 23(48): 5773-5778.
[113] Zheng H X, Chen H J, Ng J, et al. Optical gradient force in the absence of light intensity gradient[J]. Physical Review B, 2021, 103(3): 035103.
[114] Chen H J, Wang N, Lu W L, et al. Tailoring azimuthal optical force on lossy chiral particles in Bessel beams[J]. Physical Review A, 2014, 90(4): 043850.
[115] Yamanishi J, Ahn H Y, Yamane H, et al. Optical gradient force on chiral particles[J]. Science Advances, 2022, 8(38): eabq2604.
[116] Bliokh K Y, Niv A, Kleiner V, et al. Geometrodynamics of spinning light[J]. Nature Photonics, 2008, 2: 748-753.
[117] Hosten O, Kwiat P. Observation of the spin Hall effect of light via weak measurements[J]. Science, 2008, 319(5864): 787-790.
[118] Ling X H, Zhou X X, Huang K, et al. Recent advances in the

spin Hall effect of light[J]. Reports on Progress in Physics, 2017, 80(6): 066401.
[119] Aiello A, Lindlein N, Marquardt C, et al. Transverse angular momentum and geometric spin Hall effect of light[J]. Physical Review Letters, 2009, 103(10): 100401.
[120] Bliokh K Y, Smirnova D, Nori F. Quantum spin Hall effect of light[J]. Science, 2015, 348(6242): 1448-1451.
[121] Kalhor F, Thundat T, Jacob Z. Universal spin-momentum locked optical forces[J]. Applied Physics Letters, 2016, 108(6): 061102.
[122] Van Mechelen T, Jacob Z. Universal spin-momentum locking of evanescent waves[J]. Optica, 2016, 3(2): 118-126.
[123] Shi P, Du L P, Li C C, et al. Transverse spin dynamics in structured electromagnetic guided waves[J]. Proceedings of the National Academy of Sciences of the United States of America, 2021, 118(6): e2018816118.
[124] Li Y, Rui G H, Zhou S C, et al. Enantioselective optical trapping of chiral nanoparticles using a transverse optical needle field with a transverse spin[J]. Optics Express, 2020, 28(19): 27808-27822.
[125] Alizadeh M H, Reinhard B M. Dominant chiral optical forces in the vicinity of optical nanofibers[J]. Optics Letters, 2016, 41(20): 4735-4738.
[126] Alizadeh M H, Reinhard B M. Emergence of transverse spin in optical modes of semiconductor nanowires[J]. Optics Express, 2016, 24(8): 8471-8479.
[127] Chen H J, Jiang Y K, Wang N, et al. Lateral optical force on paired chiral nanoparticles in linearly polarized plane waves[J]. Optics Letters, 2015, 40(23): 5530-5533.
[128] Liu X G, Li J Q, Zhang Q, et al. Separation of chiral enantiomers by optical force and torque induced by tightly focused vector polarized hollow beams[J]. Physical Chemistry Chemical Physics: PCCP, 2019, 21(28): 15339-15345.
[129] Li M M, Yan S H, Zhang Y N, et al. Optical sorting of small chiral particles by tightly focused vector beams[J]. Physical Review A, 2019, 99(3): 033825.
[130] Li M M, Yan S H, Zhang Y N, et al. Optical separation and discrimination of chiral particles by vector beams with orbital angular momentum[J]. Nanoscale Advances, 2021, 3(24): 6897-6902.
[131] Li M M, Yan S H, Zhang Y N, et al. Orbital angular momentum in optical manipulations[J]. Journal of Optics, 2022, 24(11): 114001.
[132] Cameron R P, Barnett S M, Yao A M. Discriminatory optical force for chiral molecules[J]. New Journal of Physics, 2014, 16(1): 013020.
[133] Yesharim O, Karnieli A, Jackel S, et al. Observation of the all-optical Stern-Gerlach effect in nonlinear optics[J]. Nature Photonics, 2022, 16: 582-587.
[134] Kravets N, Aleksanyan A, Brasselet E. Chiral optical stern-gerlach Newtonian experiment[J]. Physical Review Letters, 2019, 122(2): 024301.
[135] Canaguier-Durand A, Genet C. Plasmonic lateral forces on chiral spheres[J]. Journal of Optics, 2016, 18(1): 015007.
[136] Mu X J, Hu L, Cheng Y Q, et al. Chiral surface plasmon-enhanced chiral spectroscopy: principles and applications[J]. Nanoscale, 2021, 13(2): 581-601.
[137] Cao T, Qiu Y M. Lateral sorting of chiral nanoparticles using Fano-enhanced chiral force in visible region[J]. Nanoscale, 2018, 10(2): 566-574.
[138] Alizadeh M H, Reinhard B M. Plasmonically enhanced chiral optical fields and forces in achiral split ring resonators[J]. ACS Photonics, 2015, 2(3): 361-368.
[139] Zhao Y, Saleh A A E, van de Haar M A, et al. Nanoscopic control and quantification of enantioselective optical forces[J]. Nature Nanotechnology, 2017, 12(11): 1055-1059.
[140] Ali R, Pinheiro F A, Dutra R S, et al. Enantioselective manipulation of single chiral nanoparticles using optical tweezers[J]. Nanoscale, 2020, 12(8): 5031-5037.
[141] Fang L, Wang J. Optical trapping separation of chiral nanoparticles by subwavelength slot waveguides[J]. Physical Review Letters, 2021, 127(23): 233902.
[142] Andrén D, Baranov D G, Jones S, et al. Microscopic metavehicles powered and steered by embedded optical metasurfaces[J]. Nature Nanotechnology, 2021, 16(9): 970-974.
[143] Tong L M, Miljković V D, Käll M. Alignment, rotation, and spinning of single plasmonic nanoparticles and nanowires using polarization dependent optical forces[J]. Nano Letters, 2010, 10(1): 268-273.
[144] Xu X H, Cheng C, Zhang Y, et al. Scattering and extinction torques: how plasmon resonances affect the orientation behavior of a nanorod in linearly polarized light[J]. The Journal of Physical Chemistry Letters, 2016, 7(2): 314-319.
[145] Padgett M, Bowman R. Tweezers with a twist[J]. Nature Photonics, 2011, 5: 343-348.
[146] 申泽, 成煜, 邓洪昌, 等. 鸟喙形环形芯光纤光镊粒子捕获受力分析[J]. 光学学报, 2021, 41(18): 1808001.
Shen Z, Cheng Y, Deng H C, et al. Analysis of trapping force of beak-shaped optical tweezers with annular core fibers for particles[J]. Acta Optica Sinica, 2021, 41(18): 1808001.
[147] Nieto-Vesperinas M, Xu X H. The complex Maxwell stress tensor theorem: the imaginary stress tensor and the reactive strength of orbital momentum. A novel scenery underlying electromagnetic optical forces[J]. Light, Science & Applications, 2022, 11(1): 297.
[148] Zeng J W, Wang J. Interrogating imaginary optical force by the complex Maxwell stress tensor theorem[J]. Light, Science & Applications, 2023, 12(1): 20.
[149] Zhao Y Q, Shapiro D, McGloin D, et al. Direct observation of the transfer of orbital angular momentum to metal particles from a focused circularly polarized Gaussian beam[J]. Optics Express, 2009, 17(25): 23316-23322.
[150] Bliokh K Y, Ostrovskaya E A, Alonso M A, et al. Spin-to-orbital angular momentum conversion in focusing, scattering, and imaging systems[J]. Optics Express, 2011, 19(27): 26132-26149.
[151] Kostina N A, Kislov D A, Ivinskaya A N, et al. Nano-scale tunable optical binding mediated by hyperbolic metamaterials[J]. ACS Photonics, 2019, 7(2): 425-433.
[152] Paul N K, Correas-Serrano D, Gomez-Diaz J S. Giant lateral optical forces on Rayleigh particles near hyperbolic and extremely anisotropic metasurfaces[J]. Physical Review B, 2019, 99(12): 121408.
[153] Ivinskaya A, Petrov M I, Bogdanov A A, et al. Plasmon-assisted optical trapping and anti-trapping[J]. Light, Science & Applications, 2017, 6(5): e16258.
[154] Huang S Y, Zhang G L, Wang Q, et al. Spin-to-orbital angular momentum conversion via light intensity gradient[J]. Optica, 2021, 8(9): 1231-1236.
[155] Zhang H, Gu M, Jiang X D, et al. An optical neural chip for implementing complex-valued neural network[J]. Nature Communications, 2021, 12(1): 457.
[156] Zhu H H, Zou J, Zhang H, et al. Space-efficient optical computing with an integrated chip diffractive neural network[J]. Nature Communications, 2022, 13(1): 1044.
[157] Lin L H, Peng X L, Mao Z M, et al. Bubble-pen lithography[J]. Nano Letters, 2016, 16(1): 701-708.
[158] Setoura K, Ito S, Miyasaka H. Stationary bubble formation and Marangoni convection induced by CW laser heating of a single gold nanoparticle[J]. Nanoscale, 2017, 9(2): 719-730.
[159] Kollipara P S, Mahendra R, Li J G, et al. Bubble-pen lithography: fundamentals and applications[J]. Aggregate, 2022, 3(4): e189.

[160] Lin L H, Hill E H, Peng X L, et al. Optothermal manipulations of colloidal particles and living cells[J]. Accounts of Chemical Research, 2018, 51(6): 1465-1474.

[161] Li J G, Zheng Y B. Optothermally assembled nanostructures[J]. Accounts of Materials Research, 2021, 2(5): 352-363.

[162] Ghosh S, Ranjan A D, Das S, et al. Directed self-assembly driven mesoscale lithography using laser-induced and manipulated microbubbles: complex architectures and diverse applications[J]. Nano Letters, 2021, 21(1): 10-25.

[163] Kim Y, Ding H R, Zheng Y B. Enhancing surface capture and sensing of proteins with low-power optothermal bubbles in a biphasic liquid[J]. Nano Letters, 2020, 20(10): 7020-7027.

[164] Monisha K, Suresh K, Bankapur A, et al. Optical printing of plasmonic nanoparticles for SERS studies of analytes and thermophoretically trapped biological cell[J]. Sensors and Actuators B: Chemical, 2023, 377: 133047.

[165] An S Z, Ranaweera R, Luo L. Harnessing bubble behaviors for developing new analytical strategies[J]. Analyst, 2020, 145(24): 7782-7795.

[166] Wang H, Xu B B, Zhang Y L, et al. Light-driven magnetic encoding for hybrid magnetic micromachines[J]. Nano Letters, 2021, 21(4): 1628-1635.

[167] Zhou Y T, Dai L G, Jiao N D. Review of bubble applications in microrobotics: propulsion, manipulation, and assembly[J]. Micromachines, 2022, 13(7): 1068.

[168] Karim F, Vasquez E S, Sun Y, et al. Optothermal microbubble assisted manufacturing of nanogap-rich structures for active chemical sensing[J]. Nanoscale, 2019, 11(43): 20589-20597.

[169] Piazza R. Thermophoresis: moving particles with thermal gradients[J]. Soft Matter, 2008, 4(9): 1740-1744.

[170] Gargiulo J, Brick T, Violi I L, et al. Understanding and reducing photothermal forces for the fabrication of Au nanoparticle dimers by optical printing[J]. Nano Letters, 2017, 17(9): 5747-5755.

[171] Chen J J, Zeng Y J, Zhou J, et al. Optothermophoretic flipping method for biomolecule interaction enhancement[J]. Biosensors and Bioelectronics, 2022, 204: 114084.

[172] Duhr S, Braun D. Why molecules move along a temperature gradient[J]. Proceedings of the National Academy of Sciences of the United States of America, 2006, 103(52): 19678-19682.

[173] Schermer R T, Olson C C, Coleman J P, et al. Laser-induced thermophoresis of individual particles in a viscous liquid[J]. Optics Express, 2011, 19(11): 10571-10586.

[174] Saxton R L, Ranz W E. Thermal force on an aerosol particle in a temperature gradient[J]. Journal of Applied Physics, 1952, 23 (8): 917-923.

[175] Bregulla A P, Würger A, Günther K, et al. Thermo-osmotic flow in thin films[J]. Physical Review Letters, 2016, 116(18): 188303.

[176] Wang X, Liu M C, Jing D W, et al. Net unidirectional fluid transport in locally heated nanochannel by thermo-osmosis[J]. Nano Letters, 2020, 20(12): 8965-8971.

[177] Zhou J X, Dai X Q, Peng Y H, et al. Low-temperature optothermal nanotweezers[J]. Nano Research, 2023, 16(5): 7710-7715.

[178] Roxworthy B J, Bhuiya A M, Vanka S P, et al. Understanding and controlling plasmon-induced convection[J]. Nature Communications, 2014, 5: 3173.

[179] Park J, Lee S, Lee H, et al. Colloidal multiscale assembly via photothermally driven convective flow for sensitive in-solution plasmonic detections[J]. Small, 2022, 18(24): e2201075.

[180] Jin C M, Lee W, Kim D, et al. Photothermal convection lithography for rapid and direct assembly of colloidal plasmonic nanoparticles on generic substrates[J]. Small, 2018, 14(45): e1803055.

[181] Huang J S, Yang Y T. Origin and future of plasmonic optical tweezers[J]. Nanomaterials, 2015, 5(2): 1048-1065.

[182] Ma C P, Yu P, Wang W H, et al. Chiral optofluidics with a plasmonic metasurface using the photothermal effect[J]. ACS Nano, 2021, 15(10): 16357-16367.

[183] Wang K, Crozier K B. Plasmonic trapping with a gold nanopillar [J]. Chemphyschem, 2012, 13(11): 2639-2648.

[184] Singh P, Joseph D D. Fluid dynamics of floating particles[J]. Journal of Fluid Mechanics, 2005, 530: 31-80.

[185] Stoev I D, Seelbinder B, Erben E, et al. Highly sensitive force measurements in an optically generated, harmonic hydrodynamic trap[J]. eLight, 2021, 1(1): 7.

[186] Shi Y Z, Zhu T T, Nguyen K T, et al. Optofluidic microengine in a dynamic flow environment via self-induced back-action[J]. ACS Photonics, 2020, 7(6): 1500-1507.

[187] Lü H L, Chen X Y, Wang X Y, et al. A novel study on a micromixer with Cantor fractal obstacle through grey relational analysis[J]. International Journal of Heat and Mass Transfer, 2022, 183: 122159.

[188] Ndukaife J C, Kildishev A V, Nnanna A G A, et al. Long-range and rapid transport of individual nano-objects by a hybrid electrothermoplasmonic nanotweezer[J]. Nature Nanotechnology, 2016, 11(1): 53-59.

[189] Chen X Y, Lv H L. Intelligent control of nanoparticle synthesis on microfluidic chips with machine learning[J]. NPG Asia Materials, 2022, 14: 69.

[190] Peng X L, Chen Z H, Kollipara P S, et al. Opto-thermoelectric microswimmers[J]. Light, Science & Applications, 2020, 9: 141.

[191] Lin L H, Wang M S, Peng X L, et al. Opto-thermoelectric nanotweezers[J]. Nature Photonics, 2018, 12(4): 195-201.

[192] Lin L H, Zhang J L, Peng X L, et al. Opto-thermophoretic assembly of colloidal matter[J]. Science Advances, 2017, 3(9): e1700458.

[193] Wang M S, Hu G W, Chand S, et al. Spin-orbit-locked hyperbolic polariton vortices carrying reconfigurable topological charges[J]. eLight, 2022, 2(1): 12.

[194] Qin H Y, Shi Y Z, Su Z P, et al. Exploiting extraordinary topological optical forces at bound states in the continuum[J]. Science Advances, 2022, 8(49): eade7556.

[195] Silveirinha M G, Gangaraj S A H, Hanson G W, et al. Fluctuation-induced forces on an atom near a photonic topological material[J]. Physical Review A, 2018, 97(2): 022509.

[196] Gangaraj S A H, Hanson G W, Antezza M, et al. Spontaneous lateral atomic recoil force close to a photonic topological material [J]. Physical Review B, 2018, 97(20): 201108.

[197] Paul N K, Gomez-Diaz J S. Lateral recoil optical forces on nanoparticles near nonreciprocal surfaces[J]. Physical Review B, 2023, 107(3): 035417.

[198] Gangaraj S A H, Monticone F. Coupled topological surface modes in gyrotropic structures: Green's function analysis[J]. IEEE Antennas and Wireless Propagation Letters, 2018, 17 (11): 1993-1997.

[199] Gangaraj S A H, Hanson G W. Topologically protected unidirectional surface states in biased ferrites: duality and application to directional couplers[J]. IEEE Antennas and Wireless Propagation Letters, 2017, 16: 449-452.

[200] Gangaraj S A H, Monticone F. Topologically-protected one-way leaky waves in nonreciprocal plasmonic structures[J]. Journal of Physics: Condensed Matter, 2018, 30(10): 104002.

[201] Gangaraj S A H, Hanson G W, Silveirinha M G, et al. Unidirectional and diffractionless surface plasmon polaritons on three-dimensional nonreciprocal plasmonic platforms[J]. Physical Review B, 2019, 99(24): 245414.

[202] Kingsley-Smith J J, Picardi M F, Wei L, et al. Optical forces from near-field directionalities in planar structures[J]. Physical

Review B, 2019, 99(23): 235410.
[203] Li Z, Zhang S, Tong L, et al. Ultrasensitive size-selection of plasmonic nanoparticles by Fano interference optical force[J]. ACS Nano, 2014, 8(1): 701-708.
[204] Cao T, Bao J X, Mao L B. Switching of giant lateral force on sub-10 nm particle using phase-change nanoantenna[J]. Advanced Theory and Simulations, 2018, 1(2): 1700027.
[205] Cipparrone G, Hernandez R J, Pagliusi P, et al. Magnus force effect in optical manipulation[J]. Physical Review A, 2011, 84 (1): 015802.
[206] Huggins E R. Exact Magnus-force formula for three-dimensional fluid-core vortices[J]. Physical Review A, 1970, 1 (2): 327-331.
[207] Weidman P D, Herczynski A. On the inverse Magnus effect in free molecular flow[J]. Physics of Fluids, 2004, 16(2): L9-L12.
[208] Saffman P G. The lift on a small sphere in a slow shear flow[J]. Journal of Fluid Mechanics, 1965, 22: 385-400.
[209] Tian F, Cai L L, Chang J Q, et al. Label-free isolation of rare tumor cells from untreated whole blood by interfacial viscoelastic microfluidics[J]. Lab on a Chip, 2018, 18(22): 3436-3445.
[210] Mema I, Mahajan V V, Fitzgerald B W, et al. Effect of lift force and hydrodynamic torque on fluidisation of non-spherical particles[J]. Chemical Engineering Science, 2019, 195: 642-656.
[211] Guzniczak E, Otto O, Whyte G, et al. Deformability-induced lift force in spiral microchannels for cell separation[J]. Lab on a Chip, 2020, 20(3): 614-625.
[212] Geislinger T M, Franke T. Hydrodynamic lift of vesicles and red blood cells in flow: from Fåhræus & Lindqvist to microfluidic cell sorting[J]. Advances in Colloid and Interface Science, 2014, 208: 161-176.
[213] Hejazian M, Li W H, Nguyen N T. Lab on a chip for continuous-flow magnetic cell separation[J]. Lab on a Chip, 2015, 15(4): 959-970.
[214] Kuntaegowdanahalli S S, Bhagat A A S, Kumar G, et al. Inertial microfluidics for continuous particle separation in spiral microchannels[J]. Lab on a Chip, 2009, 9(20): 2973-2980.
[215] Baumgartl J, Mazilu M, Dholakia K. Optically mediated particle clearing using Airy wavepackets[J]. Nature Photonics, 2008, 2: 675-678.
[216] Kuo H Y, Vyas S, Chu C H, et al. Cubic-phase metasurface for three-dimensional optical manipulation[J]. Nanomaterials, 2021, 11(7): 1730.
[217] Zheng Z, Zhang B F, Chen H, et al. Optical trapping with focused Airy beams[J]. Applied Optics, 2011, 50(1): 43-49.
[218] MacDonald M P, Paterson L, Volke-Sepulveda K, et al. Creation and manipulation of three-dimensional optically trapped structures[J]. Science, 2002, 296(5570): 1101-1103.
[219] Donato M G, Brzobohatý O, Simpson S H, et al. Optical trapping, optical binding, and rotational dynamics of silicon nanowires in counter-propagating beams[J]. Nano Letters, 2019, 19(1): 342-352.
[220] Yang Y J, Ren Y X, Chen M Z, et al. Optical trapping with structured light: a review[J]. Advanced Photonics, 2021, 3(3): 034001.
[221] Nedev S, Carretero-Palacios S, Kühler P, et al. An optically controlled microscale elevator using plasmonic Janus particles[J]. ACS Photonics, 2015, 2(4): 491-496.
[222] Liu J, Guo H L, Li Z Y. Self-propelled round-trip motion of Janus particles in static line optical tweezers[J]. Nanoscale, 2016, 8(47): 19894-19900.
[223] Liu Y Y, Edmond K V, Curran A, et al. Core-shell particles for simultaneous 3D imaging and optical tweezing in dense colloidal materials[J]. Advanced Materials, 2016, 28(36): 8001-8006.
[224] Rodríguez-Sevilla P, Prorok K, Bednarkiewicz A, et al. Optical forces at the nanoscale: size and electrostatic effects[J]. Nano Letters, 2018, 18(1): 602-609.
[225] Ding L, Shan X C, Wang D J, et al. Lanthanide ion resonance-driven Rayleigh scattering of nanoparticles for dual-modality interferometric scattering microscopy[J]. Advanced Science, 2022, 9(32): e2203354.
[226] Lee Y E, Fung K H, Jin D F, et al. Optical torque from enhanced scattering by multipolar plasmonic resonance[J]. Nanophotonics, 2014, 3(6): 343-350.
[227] Shi Y Z, Zhou L M, Liu A Q, et al. Superhybrid mode-enhanced optical torques on Mie-resonant particles[J]. Nano Letters, 2022, 22(4): 1769-1777.
[228] Shi Y Z, Zhu T T, Liu A Q, et al. Inverse optical torques on dielectric nanoparticles in elliptically polarized light waves[J]. Physical Review Letters, 2022, 129(5): 053902.
[229] Fujiwara H, Yamauchi K, Wada T, et al. Optical selection and sorting of nanoparticles according to quantum mechanical properties[J]. Science Advances, 2021, 7(3): eabd9551.
[230] Balthasar Mueller J P, Rubin N A, Devlin R C, et al. Metasurface polarization optics: independent phase control of arbitrary orthogonal states of polarization[J]. Physical Review Letters, 2017, 118(11): 113901.
[231] Yu N F, Genevet P, Kats M A, et al. Light propagation with phase discontinuities: generalized laws of reflection and refraction [J]. Science, 2011, 334(6054): 333-337.
[232] Lin D M, Fan P Y, Hasman E, et al. Dielectric gradient metasurface optical elements[J]. Science, 2014, 345(6194): 298-302.
[233] Ren H R, Briere G, Fang X Y, et al. Metasurface orbital angular momentum holography[J]. Nature Communications, 2019, 10(1): 2986.
[234] Song Q H, Odeh M, Zúñiga-Pérez J, et al. Plasmonic topological metasurface by encircling an exceptional point[J]. Science, 2021, 373(6559): 1133-1137.
[235] Deng Z L, Li G X. Metasurface optical holography[J]. Materials Today Physics, 2017, 3: 16-32.
[236] Zheng G X, Mühlenbernd H, Kenney M, et al. Metasurface holograms reaching 80% efficiency[J]. Nature Nanotechnology, 2015, 10: 308-312.
[237] Ni X J, Kildishev A V, Shalaev V M. Metasurface holograms for visible light[J]. Nature Communications, 2013, 4: 2807.
[238] Li L L, Zhao H T, Liu C, et al. Intelligent metasurfaces: control, communication and computing[J]. eLight, 2022, 2 (1): 7.
[239] Lee D, So S, Hu G W, et al. Hyperbolic metamaterials: fusing artificial structures to natural 2D materials[J]. eLight, 2022, 2 (1): 1.
[240] Wu X F, Ehehalt R, Razinskas G, et al. Light-driven microdrones[J]. Nature Nanotechnology, 2022, 17(5): 477-484.
[241] Li T Y, Kingsley-Smith J J, Hu Y H, et al. Reversible lateral optical force on phase-gradient metasurfaces for full control of metavehicles[J]. Optics Letters, 2023, 48(2): 255-258.
[242] Liu Y R, Ding H R, Li J G, et al. Light-driven single-cell rotational adhesion frequency assay[J]. eLight, 2022, 2(1): 13.
[243] Xin H B, Li Y C, Liu Y C, et al. Optical forces: from fundamental to biological applications[J]. Advanced Materials, 2020, 32(37): 2001994.
[244] 王秀芳, 刘旭, 董太极, 等. 用于可控式粒子捕获和轴向往复运动的电流调制型单光纤光镊[J]. 光学学报, 2023, 43(14): 1406003.
Wang X F, Liu X, Dong T J, et al. Current-modulated single fiber optical tweezers for controlled particle capture and axial reciprocating motion[J]. Acta Optica Sinica, 2023, 43(14): 1406003.
[245] Bégin J L, Jain A, Parks A, et al. Nonlinear helical dichroism in chiral and achiral molecules[J]. Nature Photonics, 2023, 17:

82-88.

[246] Pu L. Enantioselective fluorescent sensors: a tale of BINOL[J]. Accounts of Chemical Research, 2012, 45(2): 150-163.

[247] Genet C. Chiral light-chiral matter interactions: an optical force perspective[J]. ACS Photonics, 2022, 9(2): 319-332.

[248] Milonni P W, Boyd R W. Momentum of light in a dielectric medium[J]. Advances in Optics and Photonics, 2010, 2(4): 519-553.

[249] Kajorndejnukul V, Ding W Q, Sukhov S, et al. Linear momentum increase and negative optical forces at dielectric interface[J]. Nature Photonics, 2013, 7: 787-790.

[250] Qiu C W, Ding W Q, Mahdy M R C, et al. Photon momentum transfer in inhomogeneous dielectric mixtures and induced tractor beams[J]. Light: Science & Applications, 2015, 4(4): e278.

[251] Pfeifer R N C, Nieminen T A, Heckenberg N R, et al. Colloquium: momentum of an electromagnetic wave in dielectric media[J]. Reviews of Modern Physics, 2007, 79(4): 1197-1216.

[252] Nelson D F. Momentum, pseudomomentum, and wave momentum: toward resolving the Minkowski-Abraham controversy[J]. Physical Review A, 1991, 44(6): 3985-3996.

[253] Ashkin A. Applications of laser radiation pressure[J]. Science, 1980, 210(4474): 1081-1088.

[254] Baxter C, Loudon R. Radiation pressure and the photon momentum in dielectrics[J]. Journal of Modern Optics, 2010, 57(10): 830-842.

[255] Letokhov V S, Minogin V G. Laser radiation pressure on free atoms[J]. Physics Reports, 1981, 73(1): 1-65.

[256] Gieseler J, Gomez-Solano J R, Magazzù A, et al. Optical tweezers: from calibration to applications: a tutorial[J]. Advances in Optics and Photonics, 2021, 13(1): 74-241.

[257] Ding W Q, Zhu T T, Zhou L M, et al. Photonic tractor beams: a review[J]. Advanced Photonics, 2019, 1(2): 024001.

[258] Nan F, Rodríguez-Fortuño F J, Yan S H, et al. Creating tunable lateral optical forces through multipolar interplay in single nanowires[J]. Nature Communications, 2023, 14(1): 6361.

[259] 朱晨俊, 宋五洲, 屈铭, 等. 硅基纳米光镊结构的热分析和捕获特性[J]. 光学学报, 2019, 39(3): 0324002.
Zhu C J, Song W Z, Qu M, et al. Thermal analysis and trapping properties of silicon-based optical nanotweezer structures[J]. Acta Optica Sinica, 2019, 39(3): 0324002.

[260] 钟义立, 彭宇航, 陈嘉杰, 等. 光致温度场光镊:原理及生物医学应用[J]. 光学学报, 2023, 43(14): 1400001.
Zhong Y L, Peng Y H, Chen J J, et al. Optical temperature field-driven tweezers: principles and biomedical applications[J]. Acta Optica Sinica, 2023, 43(14): 1400001.

[261] 荣升, 刘洪双, 钟莹, 等. 基于光力捕获金纳米立方体的拉曼光谱增强[J]. 光学学报, 2021, 41(17): 1730003.
Rong S, Liu H S, Zhong Y, et al. Enhancement of Raman spectra based on optical trapping of gold nanocubes[J]. Acta Optica Sinica, 2021, 41(17): 1730003.

[262] Liu T J, Guo C, Li W, et al. Thermal photonics with broken symmetries[J]. eLight, 2022, 2(1): 25.

[263] Bliokh K Y, Nori F. Transverse spin of a surface polariton[J]. Physical Review A, 2012, 85(6): 061801.

[264] Richards B, Wolf E, Gabor D. Electromagnetic diffraction in optical systems, II. Structure of the image field in an aplanatic system[J]. Proceedings of the Royal Society of London Series A Mathematical and Physical Sciences, 1959, 253(1274): 358-379.

[265] Eismann J S, Banzer P, Neugebauer M. Spin-orbit coupling affecting the evolution of transverse spin[J]. Physical Review Research, 2019, 1(3): 033143.

[266] Petersen J, Volz J, Rauschenbeutel A. Chiral nanophotonic waveguide interface based on spin-orbit interaction of light[J]. Science, 2014, 346(6205): 67-71.

[267] Junge C, O'Shea D, Volz J, et al. Strong coupling between single atoms and nontransversal photons[J]. Physical Review Letters, 2013, 110(21): 213604.

[268] Zhang Q, Xie Z W, Du L P, et al. Bloch-type photonic skyrmions in optical chiral multilayers[J]. Physical Review Research, 2021, 3(2): 023109.

[269] Lei X R, Yang A P, Shi P, et al. Photonic spin lattices: symmetry constraints for skyrmion and meron topologies[J]. Physical Review Letters, 2021, 127(23): 237403.

[270] Du L P, Yang A P, Zayats A V, et al. Deep-subwavelength features of photonic skyrmions in a confined electromagnetic field with orbital angular momentum[J]. Nature Physics, 2019, 15: 650-654.

[271] Lu C F, Wang B, Fang X, et al. Nanoparticle deep-subwavelength dynamics empowered by optical meron-antimeron topology[J]. Nano Letters, 2024, 24(1): 104-113.

[272] Shi Y Z, Xu X H, Nieto-Vesperinas M, et al. Advances in light transverse momenta and optical lateral forces[J]. Advances in Optics and Photonics, 2023, 15(3): 835-906.

[273] Eismann J S, Nicholls L H, Roth D J, et al. Transverse spinning of unpolarized light[J]. Nature Photonics, 2021, 15: 156-161.

[274] Neugebauer M, Eismann J S, Bauer T, et al. Magnetic and electric transverse spin density of spatially confined light[J]. Physical Review X, 2018, 8(2): 021042.

[275] Neugebauer M, Bauer T, Aiello A, et al. Measuring the transverse spin density of light[J]. Physical Review Letters, 2015, 114(6): 063901.

[276] Shi P, Du L P, Yuan X C. Spin photonics: from transverse spin to photonic skyrmions[J]. Nanophotonics, 2021, 10(16): 46.

[277] Li C C, Shi P, Du L P, et al. Mapping the near-field spin angular momenta in the structured surface plasmon polariton field[J]. Nanoscale, 2020, 12(25): 13674-13679.

[278] Rodríguez-Herrera O G, Lara D, Bliokh K Y, et al. Optical nanoprobing via spin-orbit interaction of light[J]. Physical Review Letters, 2010, 104(25): 253601.

[279] Bauer T, Orlov S, Peschel U, et al. Nanointerferometric amplitude and phase reconstruction of tightly focused vector beams[J]. Nature Photonics, 2014, 8: 23-27.

[280] 陶也, 钟伟, 吴欣怡, 等. 光力矩的基本原理及其应用[J]. 光学学报, 2023, 43(16): 1623012.
Tao Y, Zhong W, Wu X Y, et al. Optical torques: fundamentals and their applications[J]. Acta Optica Sinica, 2023, 43(16): 1623012.

Recent Progress in Optical Lateral Forces (Invited)

Shi Yuzhi[1,2,3,4*], Lai Chengxing[1,2,3,4], Yi Weicheng[1,2,3,4], Huang Haiyang[1,2,3,4], Feng Chao[1,2,3,4], He Tao[1,2,3,4], Liu Aiqun[5], Qiu Weicheng[6], Wang Zhanshan[1,2,3,4], Cheng Xinbin[1,2,3,4**]

[1]*Institute of Precision Optical Engineering, School of Physics Science and Engineering, Tongji University, Shanghai* 200092, *China*;

[2]*Key Laboratory of Advanced Micro-Structure Materials, Ministry of Education, Shanghai* 200092, *China*;

[3]*Shanghai Frontiers Science Center of Digital Optics, Shanghai* 200092, *China*;

[4]*Shanghai Professional Technical Service Platform for Full-Spectrum and High-Performance Optical Thin Film Devices and Applications, Shanghai* 200092, *China*;

[5]*Department of Electrical and Electronic Engineering, The Hong Kong Polytechnic University, Hong Kong* 999077, *China*;

[6]*Department of Electrical and Computer Engineering, National University of Singapore, Singapore* 117583, *Singapore*

Abstract

Significance Momentum is an important backbone of wave fields such as electromagnetic waves, matter waves, sound waves, and fluid waves. As the carriers of electromagnetic waves, photons possess both linear and angular momenta, which can interact with matter and generate optical forces. The technique, or "optical tweezers" which utilize optical forces to manipulate micro/nano-objects, was established by Arthur Ashkin between the 1970s and 1980s. Optical tweezers have unparalleled advantages in capturing and manipulating microscopic particles and provide new research tools for research fields such as biomedicine, physics, and chemistry. In 1997, Steven Chu, Claude Cohen-Tannoudji, and William D. Phillips won the Nobel Prize in Physics for employing optical forces to achieve atomic cooling. It was later in 2018 that Ashkin won half of the Nobel Prize in Physics for his pioneering contributions to optical tweezers and implementing them for biomedical applications.

Optical forces adopted in optical manipulation mainly include two popular types of radiation pressure and optical gradient force. The radiation pressure is the force along the direction of the Poynting vector due to the light scattering and absorption and has important applications in atomic cooling, optical sorting, and particle propulsion. The optical gradient force is the force generated by the inhomogeneous intensity or phase distribution of the light field, with great potential in numerous physical and biomedical applications.

The optical lateral force (OLF) is an extraordinary force that is perpendicular to the light propagation direction and independent of the intensity or phase gradient of the light field. It is related to the intrinsic and structural properties of light and matter. The strategy to realize an OLF is to break the system symmetry to make photons exert transverse momenta and consequently generate optical forces on particles. Since OLF was first proposed by Nori's and Chan's groups on the same day in 2014, various methods and mechanisms have been reported to configure and explore OLF, such as utilizing the spin and orbital momenta of light, coupling of light and particle chirality, spin-orbit interaction (SOI), and surface plasmon polariton (SPP).

In the past ten years, the understanding of transverse momenta and relevant light-matter interaction has reached a new stage. Transverse momentum, whether linear or angular, is closely related to OLF since the optical force is a consequence of momentum exchange or translation between light and matter. For example, transverse spin momentum, also known as the Belinfante spin momentum (BSM), or transverse spin angular momentum (SAM), can generate spin-correlated OLF. Additionally, the imaginary Poynting momentum (IPM) can also induce OLF. The chirality of particles can couple with light and generate transverse energy flux and force near the surface. The conversion of spin angular momentum to orbital angular momentum, or the so-called SOI, endows a new way to generate the OLF.

Investigations of such extraordinary transverse light momenta and OLF deepen the understanding of light-matter interactions and have tremendous applications in bidirectional enantioselective separation, meta-robots, spintronics, and quantum physics.

Progress We review the current theoretical and experimental research progress on OLF, including different mechanisms, experimental methods, and potential applications. We first introduce some fundamentals of transverse momenta, and representative mechanisms for generating OLF from both theoretical and experimental perspectives, including the BSM,

chirality, SOI, IPM, and some other effects such as heat, electricity, bubbles, and topology. Meanwhile, we review some representative applications based on OLF, such as meta-robots, particle sorting, and some other biomedical and chemical applications. Finally, we summarize this research direction and provide our vision of new physical mechanisms and more applications that may emerge in the future.

Conclusions and Prospects Momentum and force are two fundamental quantities in electromagnetics. With the innovation and burgeoning development of optical theories of transverse light momenta, mechanisms of OLF are also advancing. The optical force has also become an essential platform and effective tool for testing and validating numerous optical phenomena including transverse momenta.

Traditional optical gradient force and radiation pressure have been widely studied in the past four decades, and their technical limitations in some applications have been well comprehended. Some peculiar optical forces discovered in recent years such as the optical pulling force and OLF are playing increasingly important roles in high-precision optical manipulation. OLF provide new possibilities for nanometer-precision sorting, enantioselective separation, and minuscule momentum probing. Additionally, unprecedented advantages of metasurfaces in electromagnetic wave guidance and steering also present more possibilities for manipulating particles. Especially in recent years, with the rapid development of nanofabrication technology, a type of "meta-robot" driven by the OLF has emerged. Although it has not been implemented in practice, its interesting properties and the new degree of freedom in optical manipulation are expected to find many biomedical applications in the future, such as cargo transporting, biotherapy, and local probing. We can also envision various biological applications of OLF, such as bilaterally sorting and binding tiny bioparticles, cargo transporting using metavehicles, stretching and folding DNA and protein molecules in line-shaped beams, enantioselective separation, and high-sensitive sensing by the helical dichroism. Therefore, we can conclude that with the development of modern optics and photonics, the two interrelated quantities of momentum and force will be explored more deeply and have wide applications in material science, biophysics, quantum science, spintronics, optical manipulation, and sensing.

Key words optical lateral force; angular momentum; optical manipulation; optical spin; chiral particles